Molecular reactions at aqueous interfaces

Manuel F. Ruiz-Lopez [ID] [1 ✉], Joseph S. Francisco [ID] [2], Marilia T. C. Martins-Costa[1] and Josep M. Anglada[3]

Abstract | This Review aims to critically analyse the emerging field of chemical reactivity at aqueous interfaces. The subject has evolved rapidly since the discovery of the so-called 'on-water catalysis', alluding to the dramatic acceleration of reactions at the surface of water or at its interface with hydrophobic media. We review critical experimental studies in the fields of atmospheric and synthetic organic chemistry, as well as related research exploring the origins of life, to showcase the importance of this phenomenon. The physico-chemical aspects of these processes, such as the structure, dynamics and thermodynamics of adsorption and solvation processes at aqueous interfaces, are also discussed. We also present the basic theories intended to explain interface catalysis, followed by the results of advanced ab initio molecular-dynamics simulations. Although some topics addressed here have already been the focus of previous reviews, we aim at highlighting their interconnection across diverse disciplines, providing a common perspective that would help us to identify the most fundamental issues still incompletely understood in this fast-moving field.

Many chemical and photochemical reactions are dramatically accelerated when they occur at aqueous interfaces, in comparison to when the same reactions occur in the gas phase or bulk water. This phenomenon is now designated as 'on-water' catalysis[1]. The term chemistry 'on-water' must be understood here in a broad sense, as it refers to processes that occur at or near aqueous interfaces in oil–water emulsions and other dispersed systems, aerosols, sprays, water nanodroplets and microdroplets, as well as extended air–water interfaces, with potential implications in atmospheric, environmental, biological, prebiotic or synthetic organic chemistry, to cite the most relevant domains. Although interfaces of liquid water with either solids or biomolecules, as well as the surface of ice, share many similarities with the examples listed above, these will not be discussed in the present Review. This Review focuses on processes occurring at liquid water–vapour interfaces (or air–water interfaces) and at the interfaces of liquid water with hydrophobic media. FIGURE 1 illustrates several systems that are covered in this Review.

The reasons underlying rate acceleration at aqueous interfaces remain unclear. In contrast to bulk solvation, the formulation of a theory of interfacial solvation is still in its early stages. Furthermore, the vast variety of phenomena occurring at aqueous interfaces may imply quite different mechanisms, which often make the implementation and interpretation of experimental measurements

a complex task. The formation of hydrogen bonds with dangling protons at the interface was first proposed to explain the catalytic role of the interface[2], but many other causes can be invoked, including confinement of reagents, partial solvation, preferential orientations, curvature in nanodroplets and water-surface pH. It is worth pointing out that physico-chemical concepts that apply to bulk water are not always applicable at aqueous interfaces, as the latter are disordered systems of nanometric thickness displaying sharp configurational fluctuations. Experimental studies based on macroscopic properties such as surface tension[3,4] have provided invaluable data on interfacial thermodynamics and structural properties. However, only with the progress of non-linear second-harmonic generation and sum-frequency generation (SFG) spectroscopies[5], and other interface-sensitive molecular techniques, are the microscopic details of interfacial phenomena being elucidated. Ab initio molecular dynamics (MD) simulations and related approaches have also provided priceless information on these issues[6–8].

Nevertheless, the literature remains scattered across various fields. Several reviews have discussed different aspects of chemistry at aqueous interfaces[4,5,9–18]. Here, we provide a general discussion on the available experimental and theoretical studies that highlight the similarities between the processes occurring at various aqueous interfaces and place them in a shared perspective, which

[1]Laboratoire de Physique et Chimie Théoriques, UMR CNRS 7019, University of Lorraine, CNRS, BP 70239, Vandœuvre-lès-Nancy, France.

[2]Department of Earth and Environmental Science and Department of Chemistry, University of Pennsylvania, Philadelphia, PA, USA.

[3]Departament de Química Biològica (IQAC), CSIC, c/ Jordi Girona 18, Barcelona, Spain.
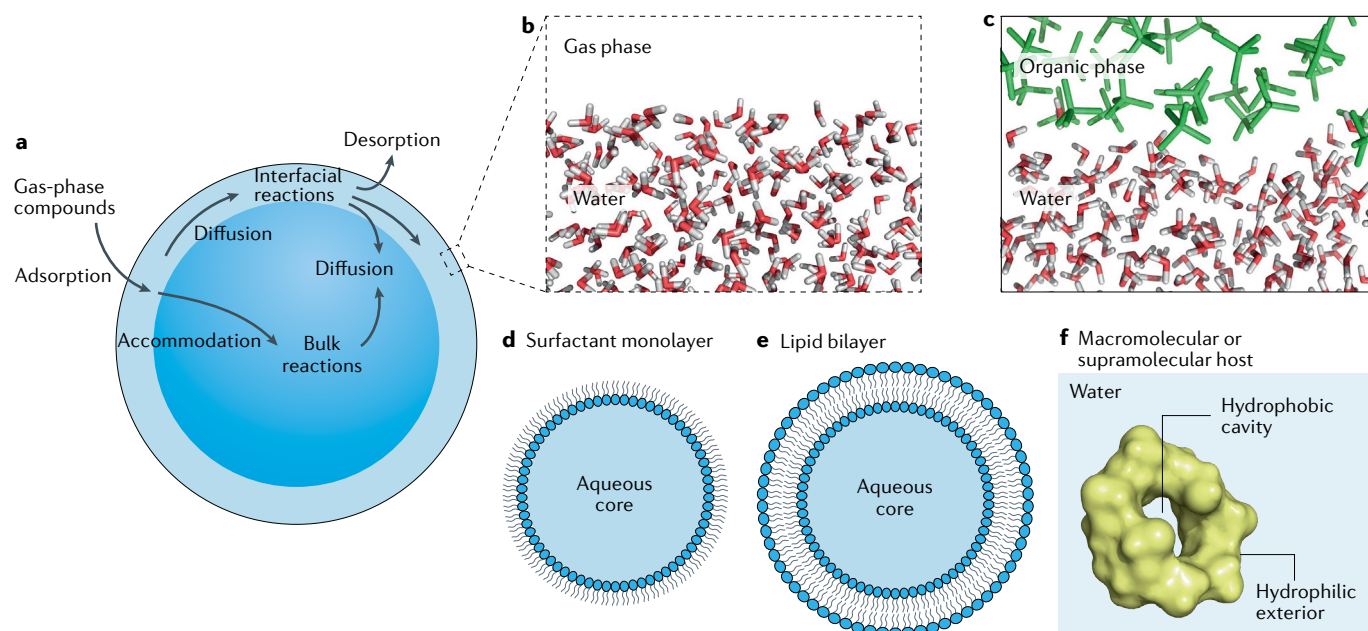
✉e-mail: Manuel.Ruiz@univ-lorraine.fr

Fig. 1 | **Examples of aqueous interfaces and interfacial processes. a** | Different processes that can take place at the air–water interface of a water droplet, such as adsorption and accommodation of compounds from the gas phase, diffusion of molecules along the aqueous interface or within the bulk reactions and desorption of the products in the gas phase. **b** | Liquid water–vapour interface. **c** | Interface of liquid water with a non-miscible organic solvent (CCl_4, in this case). **d** | Inverted micelle in aqueous organic aerosols. **e** | Vesicles. **f** | Macromolecular or supramolecular systems with a hydrophobic cavity that can host hydrophobic guest molecules. Part **a** is adapted with permission from REF.[186], Wiley.

is still lacking. In this Review, a perspective is provided through a comprehensive and critical survey of the recent literature and we point to the main challenges that need to be addressed to advance the state of the art of the field.

Chemical reactions at aqueous interfaces

Many contributions to our understanding of chemistry at aqueous interfaces are offered by the study of atmospheric chemical reactions that are found to proceed faster at the air–water interface of cloud-water droplets and aqueous aerosols than in the gas phase, influencing the atmospheric budget of trace gases[14,19–21]. The field of synthetic green chemistry has also informed us on processes at aqueous interfaces. The need to decrease the negative environmental impact of current industrial practices for the synthesis of organic compounds pleads for the use of non-organic solvents such as water. Experiments have shown that reactions in water microdroplets generated by electrospray ionization undergo remarkable acceleration with respect to bulk-phase processes, and the air–water interface is thought to play a key role because of its large surface-to-volume ratio[16,22–24]. Moreover, dispersed systems, such as polyelectrolyte solutions, micellar solutions, oil-in-water microemulsions or vesicle dispersions, have been proposed to overcome water-solubility limitations and develop biomimetic reactors within which reactions can proceed[18,25]. Aqueous interfaces have also been evoked as possible environments in which prebiotic processes could have taken place and led to the origin of life. For instance, orientation, alignment and proximity of functional groups is essential to the synthesis

of peptides by the ribosome, and air–water interfaces in inverted-micelle atmospheric aerosols or in the surface of oceans and lakes could have been a rudimentary prebiotic system mimicking this functioning[26,27].

We have selected some illustrative experimental works of chemistry at aqueous interfaces and organized them in four categories — atmospheric and environmental chemistry, reactivity in microdroplets, prebiotic chemistry and reactions at organized molecular interfaces. Despite these seeming to be disjoint areas of interest, we highlight how these categories share several similarities.

Atmospheric and environmental chemistry

The role of condensed matter in the Earth's atmosphere is widespread. Aerosols scatter sunlight and serve as seeds for the formation of clouds, which has significant consequences in climate regulation[28]. Condensed matter in its different forms can also serve as a medium for chemical transformations, such as the oxidation of SO_2 to SO_4^{2-} in water droplets, which leads to acid-rain formation in the troposphere[29], or the heterogeneous reactions that lead to ozone depletion in the stratosphere[30]. Indeed, despite a small volume fraction of atmospheric condensed matter (about 7% of the total volume of the troposphere contains clouds, and a moderately dense cloud contains about 5×10^{-7} cm³ of water per cm³ of air)[19], its relevance is now recognized[19,31,32]. It influences the atmospheric budget of trace gases through the modification of the chemical cycles of nitrogen, sulfur and various atmospheric oxidants, such as ozone[33,34]. In addition, some reaction pathways that are extremely unfavourable in

the gas phase, such as the ionic dissociations in S_N1 and S_N2 reactions, may be quite favourable in the condensed phase, producing new species[35]. Here, we put the focus on liquid-water interfaces (water droplets and aqueous aerosols), even though the heterogeneous reactions at the surface of solid matter, such as carbonaceous particles or mineral dust, have comparable importance[11,14,32].

When atmospheric trace gases interact with a water droplet, several phenomena can take place, including uptake, diffusion and reaction at the surface, desorption, mass accommodation (that is, the transfer into the bulk phase of molecules from the gas phase through their adsorption on the aqueous interface), diffusion and reaction in the bulk[36] (FIG. 1a). Bulk reactions are relatively well understood[15], but not those occurring at the air–water interface. Several studies have confirmed that the efficiency of interfacial processes in the atmosphere may be higher than bulk processes[7,11–14]. This is, in part, due to the high surface-to-volume ratio that characterizes atmospheric droplets and aerosols. However, there is evidence of specific effects that accelerate chemical and photochemical reactions at aqueous interfaces that we outline below.

The reactivity of trace organic molecules with atmospheric oxidants is enhanced when the former are absorbed on water film surfaces[12]. For example, electrospray-mass-spectrometry measurements[37] revealed that, when a benzoate ion reacts with OH radicals at the air–water interface, H abstraction from the aromatic ring provides a significant contribution (>26%) to the overall process, despite this reaction being negligible in both the gas phase and bulk water. This observation can be rationalized in terms of the destabilization of the more polar transition state for the OH-radical addition compared with H abstraction, owing to incomplete hydration at the interface[37]. A similar experimental technique was used[38] to study the reactivity of isoprene, which can undergo cationic oligomerization at mildly acidic water surfaces. The same study suggested that, at pH < 4, the air–water interface exhibits a super-acidity behaviour, a result that has raised some debate (see below).

Colussi and colleagues[39–45] have devoted considerable effort to the study of the ozonolysis reaction and the chemistry of the Criegee intermediate at the air–water interface, which are chemical processes with broad atmospheric implications, as they represent a major sink for unsaturated volatile organic compounds produced by plants, particularly isoprene and monoterpenes. One of the studies of oxidation reaction of anthracene by ozone on aqueous surfaces[46] showed that this reaction may be of comparable importance to gas-phase oxidation by OH in the atmosphere. Studies on the chemistry at the surface of sea-salt aerosols and its atmospheric implications have emphasized the role played by the air–water interface. For instance, the main sources of Cl_2 and Br_2 gases from sea-salt aerosols under dark conditions have been identified in the interfacial reactions of the corresponding halide anion with OH and O_3, respectively[47]. When concentrated NaCl aerosols are irradiated at 254 nm in the presence of O_3 to generate OH radicals, the observed amount of Cl_2 gas produced is in good agreement with

estimates based on field measurements in the marine boundary layer[20]. At the surface of aqueous aerosols, halide ions (and also some cations) influence other interfacial reactions, such as the production of NO_2 from photolysis of NO_3^- (REFS[48–50]). Some fundamental understanding of the role of water in reactions at the air–water interface of water droplets and aqueous aerosols comes from the study of small water clusters, and further details on this topic can be found in a useful perspective[51].

Photochemistry can also be enhanced at aqueous interfaces. Fatty acids, which are generally not sensitive to actinic radiation, produce aldehydes and other oxygenated species when a monolayer at the water surface is irradiated in the 280–330-nm region[21]. In the initial step, the ultraviolet absorption excites the fatty acids to a triplet state, from which they can either dissociate into radicals or react with a nearby fatty-acid molecule at the air–water interface, forming a diol radical. However, the conclusions of this study have been challenged by subsequent studies[52,53] that emphasized the need for photoinitiators for this kind of reaction to take place, as fatty acids themselves are not photoactive. Furthermore, irradiation of nebulized aqueous pyruvic acid in a simulation chamber at high-relative-humidity conditions has been shown to lead to the formation of, among other products, zymonic acid[54], which is not observed in the gas-phase or aqueous-phase photolysis of pyruvic acid, suggesting that it could be generated by reactions at the droplet surface. Other interesting interface-assisted photochemical processes have also been reviewed[14].

Microdroplets as synthetic chemical reactors

Microdroplets are emerging as efficient reactors for organic syntheses. That many organic reactions can be accelerated in aqueous media has been known for decades[55–58], especially after the seminal work by Breslow and colleagues on the acceleration of the Diels–Alder reaction[59,60]. This is rather good news because one could consider water as the ideal green solvent. Some reactions proceed optimally when an immiscible mixture of reactants and pure water is stirred; such processes are called on-water reactions[1]. Such processes occur in aqueous suspension and, thus, hydrophobic effects might be claimed to provide the driving-force for rate acceleration. Yet, experimental results showed that increased reaction rates are not the sole consequence of an effective concentration increase[1], and since the pioneering work of Sharpless and colleagues[1], on-water chemistry has been steadily expanding[17,61].

More recently, synthesis in microreactors has been the subject of intense research[16]. This includes studies in microdroplets generated by a variety of electrospray and spray methods[22,23,27,62–67], levitated droplets[68], thin films on surfaces[69,70] or microfluidic systems[71–74]. In many cases, the reaction rates are higher with respect to the rates of the corresponding bulk reactions (although a counterexample has also been reported)[75], but the effects responsible for such rate accelerations are still unclear. Confinement of reagents and increased concentration (owing to solvent evaporation) are probably important factors[16], but the large surface-to-volume ratio characterizing these systems also points at specific

interface effects[16,22–24]. Experimental study of competitive substituent effects in Claisen–Schmidt reactions also supported this statement[76]. Another experiment[73] using a biphasic microfluidics approach, which enables better control of the generated interfaces and water surface area, concluded that the stabilization of hydrogen bonds plays a role in decreasing the activation energy, in agreement with previous work[2] (see below).

Overall, the acceleration of the reaction rates in microdroplets is sometimes very large. For instance, the Pomeranz–Fritsch synthesis of isoquinoline in charged microdroplets generated by electrospray has been reported to be at least 10^6 times faster than in bulk[77]. Likewise, Fenton ($Fe^{2+} + H_2O_2$) and Fenton-like ($Fe^{2+} + O_3$) reactions have been found to proceed 10^3–10^4 times faster at aqueous interfaces than in bulk aqueous media because of a modified geometry of the hydration shell of Fe^{2+} (REF.[78]), which may have implications not only for advanced oxidation processes in water-treatment technologies but also in atmospheric and biological chemistries.

Other exciting results are those related to the observation of the spontaneous formation of hydrogen peroxide in sprayed water microdroplets[79]. Several possible mechanisms have been considered for this reaction, leading to the conclusion that the process occurs at or near the interface, where the intrinsic electric field is strong enough to ionize hydroxyl anions, generating hydroxyl radicals that then recombine to form H_2O_2. Although the mechanism is not fully understood, the result is quite remarkable because of the great importance of H_2O_2 in biomedical and industrial applications, and as a key compound in the atmosphere, owing to its oxidative capacity[80]. Similarly, Dakin and Baeyer–Villiger oxidations have been found to proceed in water microdroplets without the addition of any peroxides and acid or base catalysts, which are usually required if the reaction is performed in bulk water–organic phase[81].

It is worth remembering that reactions in microdroplets and electrospray-generated droplets are not only interesting from the point of view of analysis and synthesis, as mentioned above, but also to study a wide variety of problems in atmospheric[38,42,44], biomedical[82–84] or other areas in which aqueous interfaces play a central role. Moreover, possible scale-up of microdroplet chemical synthesis by heated ultrasonic nebulization opens up interesting industrial perspectives[85].

Finally, it must be noted that experiments using electrospray techniques and the interpretation of their results as consequences of purely interfacial reactions have raised some debates on the possible influence of ions[86] and reactions in the gas phase[87]. Two illustrative examples of the controversy will be commented on in the sections titled 'Prebiotic chemistry' and 'Chemical properties of the water surface'.

Prebiotic chemistry

The role played by aqueous interfaces on the chemical processes that led to the origin of life on Earth has received considerable interest in recent years[88–92]. It is explained by the fact that compartmentalization, together with the emergence of genetic materials as well as sunlight-driven processes[93], is considered to be a key prerequisite in the long journey towards protocells capable of growth, division and Darwinian evolution[92]. Colloidal systems, resulting from self-organization of amphiphilic molecules in aqueous environments, provide such suitable compartments in which complex chemical reactions could have taken place in the prebiotic era. In particular, vesicles formed in bulk waters (such as lakes and rivers) have attracted considerable attention because the amphiphilic bilayer that separates the aqueous interior from the exterior media in these structures bears a resemblance to cell membranes[18,25,88,94,95]. In such confined volumes, molecular crowding increases the probability of reactive encounters between chemical species and, at the same time, limits the diffusion of products. Hence, the synthesis of complex biomolecules required for the development of primitive living organisms is strongly favoured in this confined environment compared with similar reactions in bulk media[74]. However, molecular crowding is not the only important feature controlling the chemical reactivity inside the vesicle, and several works have emphasized the importance of the other parameters, including the molecular alignment at aqueous interfaces[4], electric charge and pH[92,94,96]. For example, experiments have shown that the polycondensation of amino acids and peptides is assisted by the lipidic bilayer, not only as a favourable environment for the reaction to take place[97,98] but also as an active acid–base catalyst[99].

Other possible prebiotic chemical reactors are the inverted-micelles structures of atmospheric organic aerosols[89–91]. In these systems, the organic content may be quite high (up to 50%) and there is direct evidence that palmitic and other fatty acids form the organic film on the exterior of marine aerosols[100,101]. Interestingly, it has been shown that the size of bacteria and viruses can be predicted from the asymmetric division of surfactant-covered atmospheric aerosols by combining atmospheric aerodynamics and gravity equations[90,91]. In the case of atmospheric aerosols, too, the role of the interface has been emphasized and supported by different studies. Infrared reflection absorption spectroscopy (IRRAS) and the Langmuir trough method have been used to observe the formation of peptide bonds during the condensation process of leucine ethyl ester in the presence of Cu^{2+} ions at the air–water interface[102]. IRRAS is a surface-sensitive infrared spectroscopic technique that probes the vibrations of molecules in the vicinity of the surface. In these experiments, IRRAS has been coupled to a Langmuir trough, which, by measuring the effect of a monolayer on the surface pressure of a liquid, provides the surface pressure–area isotherm, as well as useful thermodynamic information about the interface. The studied condensation reactions are thermodynamically and kinetically unfavourable in aqueous environments, but they became favoured at the air–water interface, as evidenced by the spontaneous peptide-bond formation. The interaction of Cu^{2+} ions with the amine group of the leucine ester might play a key role by inducing an orientational change of the leucine monomers that promotes the condensation reaction. Note that the probe depth in IRRAS can be as large as 1–2 μm, which is much larger than in other interface-sensitive techniques, such

as SFG, but this probe depth was considered suitable for the reactive region of interest[102].

Spontaneous reduction of several organic molecules has also been observed in aqueous microdroplets, without assistance of reducing agents, catalysts of external charges, which could represent an essential reduction route in prebiotic conditions[103]. The mechanism of these reactions is unclear but it might involve the oxidation of OH^- at the droplet surface, similar to the spontaneous formation of H_2O_2 described above[79]. Phosphorylation processes have also been observed to proceed spontaneously in aqueous microdroplets containing a mixture of sugars and phosphoric acid, most likely because of the abatement of the entropic barrier associated with the reaction in bulk solution when the process occurs at the surface[104]. Similarly, D-ribose, phosphoric acid and a nucleobase in an aqueous microdroplet can lead to the synthesis of uridine[104] and other ribonucleosides[27]. However, the use of a different experimental set-up in which uncharged droplets are generated by an aerosol atomizer prior to ionization by a DART (direct analysis in real time) source led to different conclusions regarding the reaction between sugars and phosphoric acid[87]. Unlike in electrospray ionization, during a DART experiment, species are directly ionized in the gas phase. Moreover, the use of two aerosol atomizers allows separating the reactants into different droplets, and the reactants can only mix in the gas phase within the ionization source. Such an experimental set-up enabled the analysis of different possible sources of rate acceleration, indicating that the products previously attributed to in-droplet chemistry[104] could also originate from reactions in the gas phase, which, in some cases, may complicate the interpretation of data generated by electrosprays or their variants.

Reactions at organized molecular interfaces

Quite a variety of processes occur in systems with an organized amphiphilic interface exhibiting molecular-recognition properties, possibly featuring a binding site and compartments that can host chemical reactions. Of course, some systems described in the previous sections belong to this category, such as the vesicles hosting prebiotic chemical reactions[94,95] or the organically coated atmospheric aerosols[4,12]. Chemical reactions in biological membranes can also be considered in this case[105]. Nevertheless, the focus here is on synthetic reactions in water that mimic enzymatic catalysis and have particular interest in the prospect of green chemistry. The term 'artificial enzymes' was coined by Breslow[106,107], who introduced the use of functionalized macromolecules, mainly cyclodextrins, as water-soluble catalysts that can host a non-polar reactant guest in a hydrophobic cavity. The design of artificial enzymes, or chemzymes, is a field of intense research[108–111], which has turned into the more general design of molecular-reaction vessels. Various studies have focused on antibody catalysts or abzymes[112], functionalized nanomaterials or nanozymes[113,114], dendrimers[115,116], micellar[117] and other disperse interface-rich structures (such as polyelectrolyte solutions, microemulsions and vesicles)[18], as well as enzymes confined in small-volume environments[25].

The unprecedented efficiency of these systems to selectively catalyse chemical reactions in mild aqueous environments is continuously improving and major innovations can be expected in the near future, in a context of the development of green and sustainable chemistry as a major societal challenge. Moreover, some of these systems are not only interesting for their use as bioinspired catalysts but have important applications in photovoltaics[116] and biomedicine as drug carriers[116,117].

Solvation at the water surface

The hydrogen-bond network formed by water molecules in the liquid state confers this solvent its unique properties. At the water surface, the network is inevitably disrupted and the physical and chemical properties (such as hydrogen bonds, dipole moment and acidity) of molecules lying there differ from those in the bulk. Addressing how these changes affect chemical reactivity is a complex issue that requires a close examination of the structure and properties of the water surface. This section reviews some theoretical and experimental studies of structural (hydrogen bonding), chemical (acid–base) and solvation (dynamics and thermodynamics) properties of the liquid water–vapour interface.

Chemical properties of the water surface

The structure of the water surface has been a subject of intense debate for many years[118]. Most of the current knowledge comes from experimental studies based on SFG vibrational spectroscopy and from theoretical and computational works. The first SFG spectrum of the liquid water–vapour interface[119] showed that about 20% of water molecules display a dangling bond — the free OH bond that is projected into the vapour phase. This result was originally predicted by pioneer MD simulations[120,121] and was further confirmed and rationalized by subsequent ab initio simulations and analysis of SFG spectra[122–124]. More recent theoretical studies have also supported the idea of a 2D H-bond network at the water surface (the 'water skin') with oscillating OH bonds around a plane parallel to the instantaneous surface[125]. A schematic view of the water surface is displayed in FIG. 2, which also shows a typical density profile from classical MD simulations. The thickness of the air–water interface is usually deduced from the density profile $\rho(z)$ by fitting a function:

$$\rho(z) = \frac{\rho_o}{2}\left(1 + \tanh\left(-\frac{(Z - Z_G)}{\delta}\right)\right) \qquad (1)$$

where ρ_o is the bulk density, Z_G is the position of the Gibbs dividing surface, where $\rho(Z_G) = \frac{\rho_o}{2}$, and δ is an interface-thickness parameter related to the so-called 90–10 thickness t (that is, the thickness corresponding to a change of the water density from 90% to 10% of ρ_o) by the expression $t = 2.1972\delta$. Values of δ can change significantly with the theoretical model[9,126–128], but common values at 300 K lie in the range 1.4–1.8 Å.

The dynamics of water reorientation has been a broadly studied subject, both in bulk water[129] and at interfaces[127,130–137]. Simulations[131] and experiments using
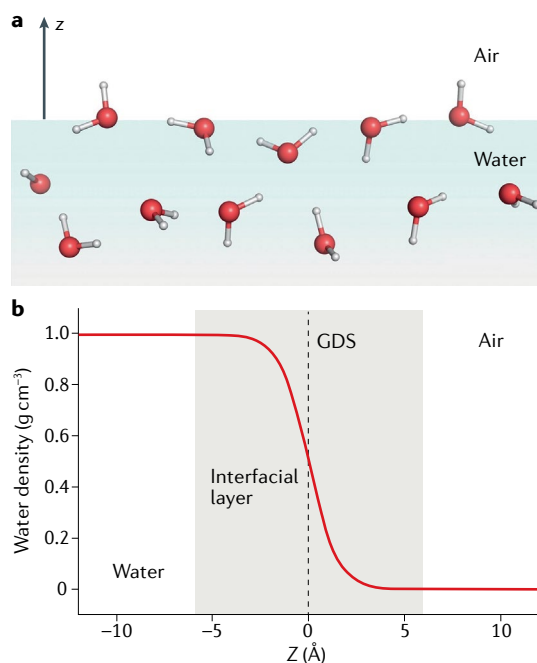
Fig. 2 | **Schematic structure of the water surface.**
a | A water surface exhibiting free OH groups pointing towards the air layer[119–124]. **b** | Typical density profile of water at the air–water interface from molecular-dynamics simulations[9,126–128]. The vertical dashed line indicates the Gibbs dividing surface (GDS), which corresponds to a water density that is half of the bulk density. The density profile corresponds to Eq. 1, with $\rho_o = 1$, $\delta = 1.5$ and $Z = 0$.

femtosecond pump–probe vibrational sum-frequency spectroscopy[130] have shown that reorientation of free OH groups of water molecules at the liquid–vapour interface takes place on a subpicosecond timescale and is about 2–3 times faster than water reorientation in the bulk[130,131].

Particularly relevant to reactivity at aqueous interfaces is the acid–base character of the water surface, an issue that remains incompletely elucidated and has raised intense controversies in the literature[138–143]. This issue is connected to the properties of water in nano-confined environments, such as inversed micelles, an aspect that we will not discuss in this Review but that has attracted a lot of attention, while it remains not completely understood[144,145]. Interestingly, experiments and calculations reveal unforeseen acid–base behaviour of aqueous interfaces. For example, HCl fully dissociates at the interface but HNO_3 maintains essentially its molecular form[146–148], unless ions are present[149], and HCOOH dissociates faster at the interface than in the bulk[150]. Vibrational-spectroscopy measurements of the ionization state of L-phenylalanine indicate a decrease of the pK_a of its polar groups at the air–water interface[151]. Depending on the experimental and theoretical technique used[138,139,141,152–161], apparent opposite conclusions have been deduced for the interface affinity of H_3O^+ and OH^- and their spatial distribution, though most recent SFG experiments on the D_2O–air interface indicate that the hydrated proton is much more surface-active than hydroxide[162]. Discordant results probably arise due to the

inherent difficulties in interpreting experiments owing to the different conditions, such as different probing depths, and by the limited accuracy of numerical simulations. Electrospray-mass-spectrometry experiments by Colussi and colleagues[38,141,153,163] led them to conclude that (in their own words): "(1) water is more extensively self-ionized at the surface than in the bulk, and (2) interfacial H_3O^+ is a stronger acid (a "superacid") and interfacial OH^- a stronger base than their bulk counterparts likely due to limited hydration"[164]. According to these authors, the acidic or basic behaviour of the surface of water would rather be interpreted in terms of the availability of proton or hydroxide ions at a given pH, with pH ~ 3 being neutral (instead of 7 as in bulk water)[141,153,165].

An enhanced autolysis of water at hydrophobic interfaces due to the strong local electric-field gradient (with an isoelectric point around pH 4) was already observed in a study aimed at explaining the contrasting observed electro-osmotic properties of microfluidic channels[166]. Calculations showed that water self-ionization is more favourable in water clusters of 20 (REF.[167]) or 21 (REF.[168]) water molecules compared with bulk solution. This unexpected result is probably a consequence of the topology of the hydrogen-bond network and could also provide some insights to the acid–base properties of water in extended aqueous interfaces. A complete survey and a comparative analysis of experimental and theoretical results collected up to 2016 can be found in REFS[142,143]. As an example of the ongoing discussion, one can refer to the experiments of isoprene oligomerization in aqueous electrosprays and mildly acidic water[38] that we have previously discussed. The reactivity of isoprene in electrosprays has been compared with that in isoprene–water emulsions at various pH values, in an attempt to differentiate between pure interfacial effects and effects caused by the experimental conditions of the electrosprays (such as charge separation and concentration of reactants)[86]. According to this study, the absence of chemical reactions in emulsions suggests that the high voltages in the electrosprays is an important parameter that leads to charge separation that facilitates the formation of partially hydrated, highly reactive H_3O^+, which then catalyses the oligomerization of isoprene. These conclusions were supported by theoretical calculations of the activation barriers for protonation and oligomerization of isoprene on $(H_3O^+)(H_2O)_n$ clusters in the same study. Clusters with $n = 3$ and $n = 36$ were selected as representative of electrospray and pristine air–water interface experiments, respectively. The results showed that the barriers are easily surmountable in the small cluster, while they are prohibited in the larger one at ambient conditions. Further works by the same groups[165,169] have debated on the effects that the partial solubility (millimolar level) of isoprene in water might have on the fate of isoprene oligomerization in the case of isoprene–water emulsions. The controversy has focused on the possibility that the diffuse nature of the interface in this case prevents the formation of partially hydrated hydronium ions that are necessary to initiate the oligomerization process, and, as a corollary, on the question: do isoprene–water emulsions correspond to the on-water or in-water category of reactions? In this respect, it is interesting to consider

the case of Huisgen cycloadditions, for which the endo or exo selectivity depends on the hydrophobicity of one of the reactants[61]. This was used to classify reactions as being either in-water versus on-water because on-water reactions do not display increased endo effects relative to organic solvents, in contrast to in-water reactions. To sum up, the case of isoprene oligomerization illustrates the ongoing controversies about the acidic properties of the water surface and highlights how different conclusions about interface effects on reactivity can be obtained, depending on the experimental set-up. The combined use of multiple analytical platforms and elaborated numerical simulations will be most useful to test different hypotheses and obtain more insights in this field.

Finally, analysis of the HOMO and LUMO energies and isosurfaces of a water slab using ab initio MD simulations has highlighted the increased reactivity of the water–vapour interface compared with bulk water[124].

The polarity of the water surface

Solvent polarity has been a widely used concept in chemistry to rationalize solvation phenomena[35]. Because a precise definition of solvent polarity is not straightforward, empirical parameters derived from linear Gibbs-energy relationships have been commonly used instead[35], and polarizable-continuum models based on the static dielectric constant of the solvent have been proven to be successful for the computational study of processes in bulk solution[170] and, more recently, at interfaces as well[171–173].

However, the concept of solvent polarity cannot be easily applied to understand and rationalize the solvation power of aqueous interfaces. Experimental attempts to characterize the polarity of aqueous interfaces using different second-order non-linear spectroscopies have led to conflicting results. On one hand, experiments suggested that an interface-polarity scale could be defined from the intramolecular charge-transfer absorption-band positions of the push–pull species N,N-diethyl-p-nitroaniline and 4-(2,4,6-triphenylpyridinium)-2,6-diphenylphenoxide at the liquid–liquid (water–1,2-dichloroethane and water–chlorobenzene) and air–water interfaces, respectively[174]. This interface-polarity scale would be based on a simple relationship according to which the polarity of a liquid–liquid interface corresponds to the arithmetic average of the polarity of the two bulk phases — suggesting that long-range solute–solvent interactions might have a dominant effect over local interactions at the interface. Likewise, the polarity of the air–water interface would be close to that of a low-polar solvent. On the other hand, measurements using coumarin derivatives[175] and other dyes[176,177] as polarity probes have shown the limitations of the arithmetic-average rule, claiming that the polarity of aqueous interfaces is not a well-defined concept. For example, the spectroscopic properties of dyes are greatly modified by rearrangements of their solvation shell, as illustrated in REF.[178] for $para$-nitroaniline. Therefore, the apparent polarity of the water surface depends on the position and orientation of the probe relative to the interfacial boundary, which relies on its structure, such as stereochemistry and hydrophobic groups (BOX 1).

Theoretical studies can help us to better understand interface polarity. Classical and first-principles MD simulations of glyoxal (O=CH–HC=O) have shown


Box 1 | Interface polarity

The determination of the polarity of an aqueous interface is strongly influenced by the structure of the molecular probe. According to the simple dielectric model shown in the schematic in panel **a**, when a point dipole moment μ (red arrow) approaches the sharp, planar air–water interface from gas phase, the electric field (E) generated by the solvent polarization is equal to the electric field created by its image dipole[173] (blue arrow). The reaction-field components, E_r and E_θ, depend on the distance to the dielectric surface (d), the angle (θ) between the dipole vector and the z-axis perpendicular to the surface, and the dielectric constant of water $\epsilon_w = 80$.

$$E_r = \frac{(\epsilon_w - 1)}{(\epsilon_w + 1)} \frac{2\mu \cos(\theta)}{(2d)^3}; E_\theta = \frac{(\epsilon_w - 1)}{(\epsilon_w + 1)} \frac{\mu \sin(\theta)}{(2d)^3} \qquad (2)$$

Therefore, the water-response electric field only aligns to the dipole moment for $\theta = 0$, $\pi/2$ and π. Furthermore, its modulus depends on the tilt angle as $(1 + 3\cos^2(\theta))^{1/2}$, which lies between 1 and 2 and is the same for θ and $\pi - \theta$ (up or down dipole directions). These features contrast with the case of an isotropic bulk dielectric medium.

We also schematize the case of a real molecular push–pull probe (instead of a point dipole) such as $para$-nitroaniline (panel **b**). In this case, one has to take into consideration also the finite size of the system and the chemical properties of the molecular groups. For instance, calculations for several $para$-nitroaniline–water clusters have shown that the solvation shell of the nitro and amino groups leads to a red shift and a blue shift of the electronic absorption band, respectively[178]. As a result, different absorption shifts are expected under the effect of molecular reorientations at the air–water interface (green arrows), which produce changes in the interactions with the surface (dashed red lines) and should imply conflicting conclusions about the air–water interface polarity.
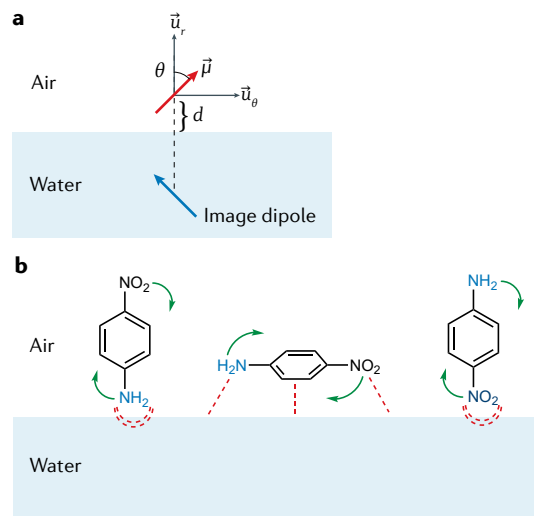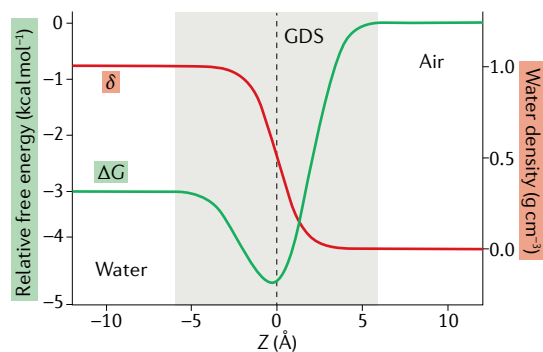

Fig. 3 | **Thermodynamics of solvation at aqueous interfaces.** Schematic plot for the relative free-energy profile (ΔG) for a neutral (water-soluble) solute crossing the air–liquid water interface. The density profile of water (δ) is also shown. The free energy decreases from the air layer (right part of the figure) to the interface, where it displays a minimum (shaded area) close to the Gibbs dividing surface (GDS, in this case for $Z = 0$, with Z being the distance of the solute from the water surface) and then increases from the interface to the bulk. Note that the width of the interface layer (shaded area) is about 1 nm. Depending on the solute's structure and its hydrophilic or hydrophobic character, the free-energy profile can display substantial differences. For example, a free-energy maximum can occur between the interfacial layer and the bulk water, and the sign of the relative air–bulk water free energy can be reversed.

that air–water and air–acetone interfaces selectively stabilize the polar *cis*-conformer (the two polar C=O bonds pointing in the same direction) over the apolar *trans*-conformer (C=O bonds pointing in opposite directions)[179,180]. This result can be explained by the fact that both stereochemistry and polarity favour the interaction of the *cis*-isomer with the interface. Stereochemistry and polarity, however, do not always go in the same direction, as in the case of *meta*-cyanophenol and *para*-cyanophenol isomers. Ab initio calculations using a dielectric model[173] show that, despite its lower polarity, the *meta*-isomer has a higher interface affinity because, in this case, the –CN and –OH groups can simultaneously interact with the aqueous layer through hydrogen bonds.

Thermodynamics and dynamics of solvation
The energetics of solvation at aqueous interfaces is a vast subject with extensive literature and a multitude of facets. Here, we focus on the aspects of this topic that are relevant for our understanding of chemical reactivity of organic compounds at air–water interfaces. In the field of atmospheric chemistry, several reviews have already been published describing the uptake and accommodation processes, the energetics of interface adsorption and the most common experimental techniques in use[4,12,36]. MD simulations have also enabled the calculation of the potential of mean force for the adsorption and accommodation processes of many chemical species. These studies have indicated a pronounced interface affinity, not only for hydrophobic or amphiphilic organic molecules[9,12,13,181,182], as expected, but of small polar systems[183–188] and even ions[189]. An archetypal

free-energy profile for moving a neutral, water-soluble compound from the gas phase to bulk water across the air–water interface is shown in FIG. 3 (the solvation of ions is considered in deeper detail below). The free energy decreases for the molecules moving from air to bulk, with a minimum at the interfacial layer. These energy profiles are useful to obtain Henry's constants and surface excess properties[183]. Theoretical analysis[182] of the solvation of organic molecules in water droplets has revealed that the surface preference is principally driven by enthalpic effects. In fact, the decomposition of the enthalpic profiles into water–water and solute–water potential energies shows that these contributions work in opposite directions to each other. In particular, when the solute is on the surface of the droplet, the water–water interaction is greater than when the solute is in the bulk (more negative energy) because of the lower disruption of the water hydrogen-bond network in the first case. This energy difference explains the presence of an energy minimum at the surface. Entropic effects further enhance the surface preference when organic molecules approaching the aqueous surface bear large apolar groups (for example, 4–5 carbon atoms or longer hydrophobic chains).

Because of the asymmetry of the aqueous interface, the dynamics of adsorbed solutes also differ from the solute dynamics in the bulk. The axial oscillations of the solute's position across the average interface plane imply concomitant fluctuations of the instantaneous hydration shell, which may be quite large compared with those in the bulk[188,190] These axial oscillations are illustrated in FIG. 4 for methanol[190] and ozone[188] at the air–water interface. Furthermore, orientational dynamics of the solute at the aqueous interface are different from those occurring in the bulk because of the existence of preferred orientations of the solute on this surface. Reorientational relaxation at the interface can be characterized by time-resolved and polarization-resolved pump–probe SFG spectroscopy[191] or by MD simulations. Calculation of the rotational autocorrelation functions of the methane derivatives MeCl, MeCN and MeOH, which are important organic compounds in the troposphere, shows that the reorientation decay times increase with the hydrogen-bonding capability of the solutes, that is, with the strength of their interface anchoring[190].

Interface affinity of ions
Ions on the outermost interface layers are more easily available to catalyse chemical reactions (for example, on sea-salt aerosols) and it is, therefore, crucial to set up a scale of their interface affinity values. Beyond that, interface affinities are valuable to establish kosmotropic (structure-making) and chaotropic (structure-breaking) scales, predict the surface tension of electrolyte solutions or explain the Hofmeister series[192,193]. In the classical view of electrolytes that considers the interface as an abrupt discontinuity between two dielectric continuum media[194], the air–water interface is devoid of ions. In such models, the point charge q in a dielectric with dielectric constant ε_1 (water) interacts with its image charge $q' = q(\varepsilon_1 - \varepsilon_2)/(\varepsilon_1 + \varepsilon_2)$ in the dielectric with constant ε_2 (air), and is, therefore, repelled from the interface for $\varepsilon_2 < \varepsilon_1$. The divergence found in this model for
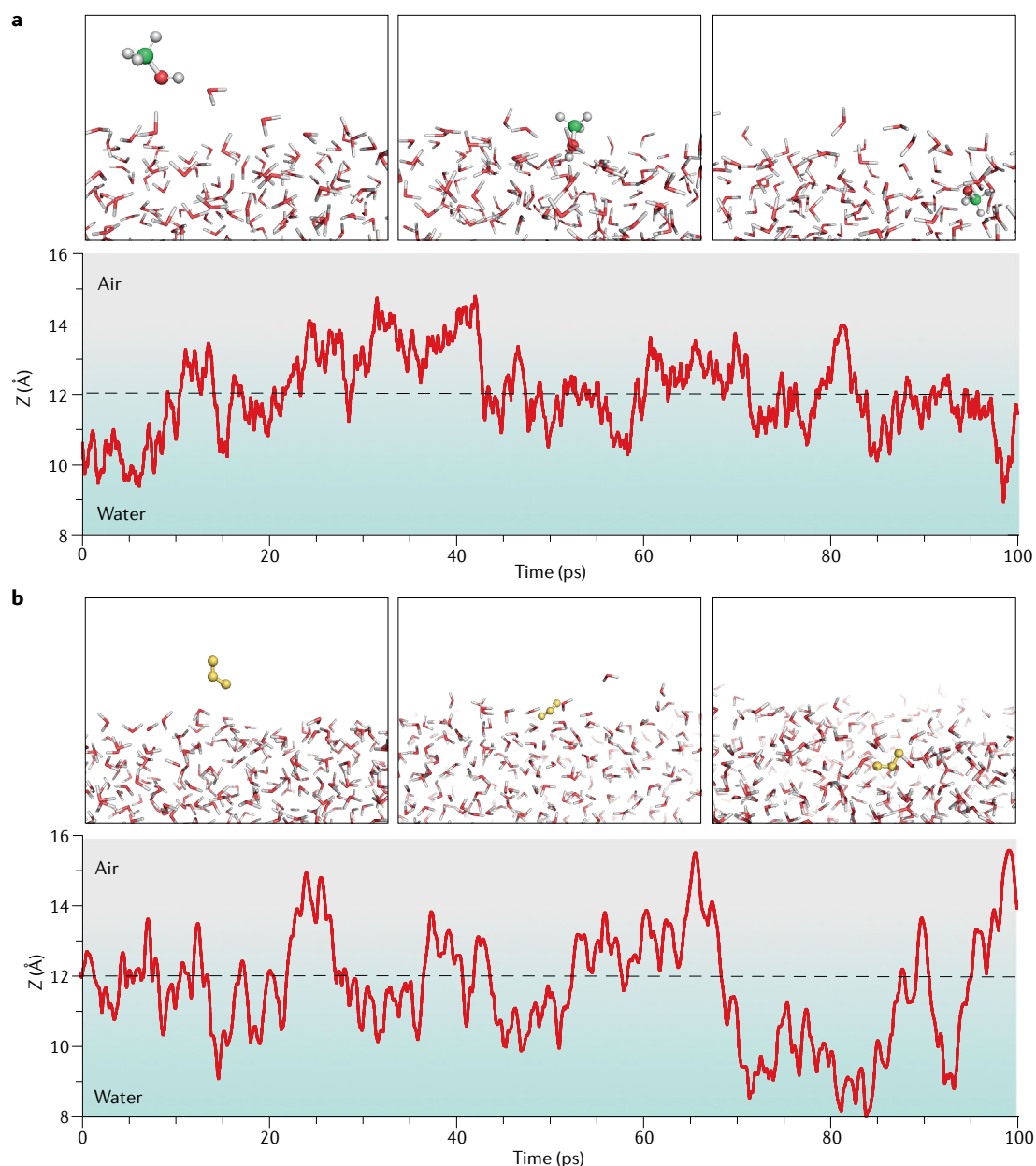
Fig. 4 | **Solute at the air–water interface. a** | Quantum mechanics/molecular mechanics molecular-dynamics simulation of the fluctuations of the methanol axial position (Z) with respect to the average interface plane (Z = 12 Å) and selected snapshots[190]. **b** | Quantum mechanics/molecular mechanics molecular-dynamics simulation of the fluctuations of the ozone axial position (Z) with respect to the average interface plane (Z = 12 Å) and selected snapshots[188]. The curves show that the fluctuations occur within a width of about ± 4 Å around the average interface. The snapshots illustrate different cases in which the solute (methanol or ozone), depending on its relative position with respect to the interface (air or water layers), is more or less hydrated. The variation of the solute's hydration shell turns into significant fluctuations of its molecular properties[188,190]. Part **a** has been replotted from data in REF.[190]. Part **b** is adapted with permission from REF.[188], PNAS.

ions approaching the interface can be untangled for finite-radii ions[195]. Although a full understanding of the interface ion affinity is still lacking, many endeavours have been made to get beyond the classical model. The macroscopic description arising from surface tension and electrostatic-potential measurements has been supplemented by data from interface-sensitive spectroscopic techniques such as SFG, by elaborated dielectric continuum theories and MD simulations, providing new insights[10,189,192,193,196–203].

Hard non-polarizable ions (such as F^- or alkali cations) and multiply charged ions (such as SO_4^{2-}) behave classically and are repelled from the interface, but large polarizable anions (such as I^- or Br^- and, to a lesser extent, Cl^-) display a propensity for the air–water interface[10,196]. The case of H_3O^+ discussed above is an exception and its interface affinity results from specific hydrogen-bonding properties[196]. Although it goes beyond the scope of this Review, the stability of the solvated electron at aqueous interfaces has also been

Box 2 | **Transition-state theory of reaction rates**

Transition-state theory is at the basis for the thermodynamical analysis of reaction rates. For a simple bimolecular reaction following a first-order rate law for reactants A and B and going through the transition complex $(AB)^{\ddagger}$:

$$A + B \rightarrow (AB)^{\ddagger} \rightarrow C \qquad (3)$$
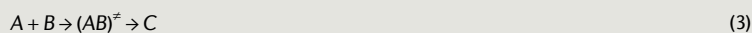
the reaction rate v is written:

$$v = -\frac{d[A]}{dt} = k[A][B] \qquad (4)$$

where the rate constant k is:

$$k = \frac{k_B T}{h} \frac{Q_{AB^{\ddagger}}}{Q_A Q_B} e^{-\frac{E_a}{RT}} = \frac{k_B T}{h} e^{\frac{-\Delta G^{\ddagger}}{RT}} \qquad (5)$$

in which Q_x represents the partition functions of solvated species x, and E_a and $\Delta G^{\ddagger}$ are the energy and free energy of activation, respectively. If one assumes equilibrium between the interfacial layer and the bulk, and compares the reaction rates in the two media, enhanced interface rates can arise from surface-enriched concentrations, lower activation energies or higher pre-exponential factors (entropy of activation). Absolute production rates will depend on the surface-to-volume ratio of the system, or, more precisely, on the ratio of the interfacial (V_i) and bulk (V_b) layer volumes. Let us figure out the order of magnitude of such a ratio. In a water droplet of diameter $1\,\mu m$ and for an interfacial-layer thickness accessible to the solute of $1.5\,nm$, $V_i/V_b \sim 10^{-10}$. Thus, equal production rates will occur if the reactants $A + B$ are stabilized by $-RT\ln(V_i/V_b)$ (same kinetic constant assumed), which amounts to $\sim 14\,kcal\,mol^{-1}$ at $300\,K$ (~ 3 hydrogen bonds). Similar results are obtained if the activation free energy decreases by the same amount at equal average reactant concentrations.

studied[204–206] because of potential implications in numerous chemical processes, including radiation chemistry, electron transfer, redox and electrochemical reactions.

The interface affinity of ions has been explained — at least qualitatively — by a favourable balance between electrostatic and cavitation energies[202,207,208]. The latter represents the energy cost required to disrupt water–water interactions in the medium to create a hole where the ion is placed. The cavitation energy decreases when the ion moves from bulk to the interface and for bulky soft ions, it can overcompensate the loss of favourable ion–water electrostatic interactions. In such a case, the ion stabilizes at the interface. The role of anion polarizability has been emphasized[10,189] and, though correlation with interface affinity is not always apparent[209], this term must be taken into account for a quantitative description of the adsorption energetics, as it was reported for aqueous solutions of ClO_4^- using SFG spectroscopy[208]. Under the effect of the local electric field (the permanent field arising from the asymmetry of the interface and the ion-induced reaction field), the electronic cloud of large polarizable anions is distorted and the induced dipole moment contributes to enhancing the solvation of the ion at the interface[196]. Solvation-dispersion forces may also influence interfacial adsorption[202,207], especially at oil–water interfaces[192].

Cations are dragged to the interface from the bulk through the electrostatic interactions with the anions and accumulate in nearby inner layers[196], although their distribution is quite sensitive to the type of counterions present[193]. Anions and cations interact differently with water: alkali cations are repelled from the interface because they are strongly hydrated, whereas anions

may behave either as kosmotropes or chaotropes[192]. Kosmotrope anions remain strongly hydrated in the vicinity of the interface, whereas chaotrope anions lose their hydration shell and become adsorbed to the interface. The distribution of anions and cations near the air–water interface is also influenced by the electrostatic potential originated by the orientation of water molecules at the interface, although the role of this surface potential still remains unclear[210]. Indeed, classical calculations using point-charge force fields predict the air layer to be more electropositive than water (in congruence with the image of dangling protons pointing towards the air layer), whereas explicit treatment of the electronic cloud in ab initio simulations predicts the opposite trend[189,192,211]. Thus, the anionic adsorption predicted with polarizable force fields is probably overestimated[192]. The adsorption energy of ions has been decomposed in enthalpic and entropic terms in some cases[189], and computational studies have concluded that adsorption of heavier halides is favoured by enthalpy and opposed by entropy[201,212], whereas F^- is driven to bulk by entropy[212].

Interfacial-reaction kinetics

The term 'on-water catalysis' is generally used to describe the observed rate enhancement of many chemical reactions at aqueous interfaces. In some cases, however, the apparent rate enhancement simply results from compartmentalization at the interface, for example, from an increase of reactant concentration, and not necessarily from a catalytic effect, that is, from a decrease of the activation energy (BOX 2). The rate enhancement at the interface of water microdroplets owing to compartmentalization can be described by a non-catalytic reaction–adsorption model that couples interface and bulk reactions, and accounts for interface–bulk diffusion within the droplets[74]. This model shows that the apparent forward rate constant and apparent reactants–products equilibrium constant are inversely proportional to the droplet radius, consistent with experimental data reported in the same study for a bimolecular imine synthesis[74]. But interfacial effects other than the accumulations of the reactants can also promote the reaction by lowering the activation barrier. We present below some basic theories of interface catalysis supported by experiments and/or calculations. We also discuss the results of some advanced simulations that aim at an accurate description of dynamics effects and estimate non-equilibrium solvation corrections to conventional transition-state theory in solution[213]. We focus on the neat water surface and we do not discuss the role of ions, organic layers or other species.

Basic theories of interface catalysis

Several enthalpic or entropic solvation effects may cause transition-state stabilization and reaction acceleration. We discuss some of the major effects below.

Hydrogen bonding. Dangling OH groups at the water surface have been suggested to be at the origin of 'on-water' catalysis observed for some processes[2,214]. These OH groups are available for hydrogen-bond formation with
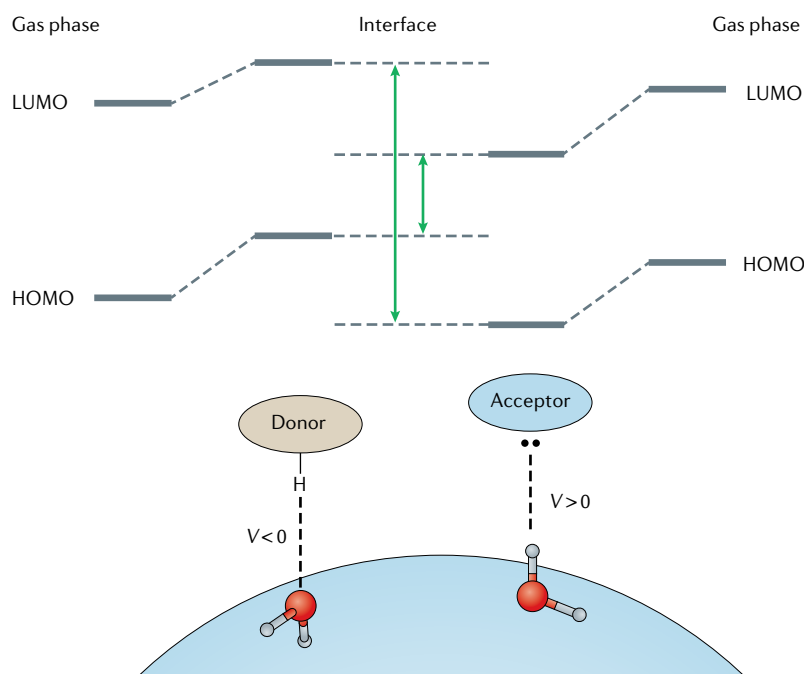
Fig. 5 | **Reactant molecular orbitals at the air–water interface.** The scheme shows how the frontier molecular orbitals, HOMO and LUMO, of proton-donor and proton-acceptor molecules are perturbed at the air–water interface. Roughly, the solvent response in the vicinity of a proton donor generates a negative electrostatic potential that destabilizes the molecular orbitals of the solute. On the contrary, the molecular orbitals of a proton acceptor are stabilized by positive electrostatic potential resulting from the solvent response. Thus, the HOMO–LUMO energy difference between the partners of a chemical reaction changes with respect to isolated molecules. This effect can be used to selectively modify the chemical reactivity. Reactions in which the proton donor behaves as a nucleophile and the proton acceptor behaves as an electrophile will be favoured. The $HO_2 + H_2CO$ reaction is an example of this kind of interface-promoted processes[187].

the chemical system along the reaction path and catalysis would occur when hydrogen bonds to the transition state become stronger than those to the reactants. It was also suggested that, although in the bulk water molecules around hydrophobic groups must first reorganize before OH groups become available for catalysis, this process is not necessary at the interface, resulting in a lower activation barrier and faster processes. Calculations for the cycloaddition reaction of quadricyclane with dimethyl azodicarboxylate, which exhibits a large acceleration on-water[214], supported this interpretation, showing that the number of hydrogen bonds with the dangling OH groups is higher for the transition states than for the reactants.

Acid–base catalysis. The acid–base properties of interfacial water can also influence and drive catalysis, notwithstanding the ongoing debate over the acidity or basicity of the water surface (see discussion above). We have discussed the electrospray-mass-spectrometry experiments[38] for the study of the oligomerization of isoprene, which suggested that surficial water is super-acidic, even for mildly acidic water solutions. Similarly, Beattie and colleagues[215] suggested that acid–base chemistry is responsible for on-water catalysis, which would be enabled thanks to the strong interface affinity

of the hydroxide ion implied by some experiments from the same group[139].

Electrostatic fields. Electric fields can drive chemical processes by modifying their rates or selectivities, as for Diels–Alder reactions[216–218]. Within the crude approximation of dielectric models, the electric field created by the dielectric response of the solvent to the charge distribution of the solute interacts with the solute, contributing to the stabilization of the whole system. Generally, processes displaying increasing polarity (charge separation) along the reaction path will be more favoured in bulk water than in the gas phase. At the interface, things are far more complicated, because the meaning of 'polarity' and its contribution to solvation are less clearly defined. Besides, standard dielectric models neglect the electric field that results from the broken symmetry of the neat water surface, the magnitude of which still does not reach general agreement[189,192,211]. It appears, therefore, difficult to establish general rules, even qualitative ones, for electrostatic-field effects on interfacial-reaction thermodynamics without undertaking a rigorous study of the microscopic structure of the system.

Reactivity indices. The frontier orbitals HOMO and LUMO, as well as other reactivity indices in density functional theory[219] (such as chemical potential, hardness and electrophilicity) are widely used to interpret or predict the fate of chemical and photochemical reactions. It has been shown that these indices are particularly sensitive to the interface electrostatic potential, which can produce larger effects than the potential in bulk water[173,186,187]. It is worth noting that these reactivity indices are highly dependent on the relative orientation of the reactant molecules with respect to the interface plane, which gives particular importance to the presence of proton donor or acceptor groups, as illustrated in FIG. 5. A good example is the case of the reaction of H_2CO (a proton acceptor) with HO_2 (a proton donor), which involves a proton-coupled electron transfer[187]. The electron transfer is favoured at the interface with respect to both gas phase and bulk water because the HOMO-(HO_2)–LUMO-(H_2CO) energy gap decreases under the local interface electrostatic potential generated by the hydrogen-bonded water molecules.

Activation entropy. Preferred orientations, hindered rotations and limited translational freedom at interfaces do also influence reaction rates through the entropy of activation. A rough model[220] for bimolecular reactions predicts a rate increase at the interface as significant as ~10^7. The model consists of a 2D interface, and assumes the same bulk and interface activation energy and the same concentrations of the two reactants, which are equal to 10^{18} molecules cm^{-3} and 10^{14} molecules cm^{-2} at the bulk and interface, respectively. According to this model, each chemical species is 'anchored' to the 2D interface and has only one translational and two rotational degrees of freedom. Hence, the loss of entropy in the activation process of a bimolecular reaction is smaller at the interface than in the bulk. The estimated rates of the quadricyclane–dimethyl

acetylenedicarboxylate cycloaddition at a water interface compared with neat reactants reflect an enhancement of two orders of magnitude, considering only the decrease of rotational degrees of freedom[214]. Despite some efforts to measure detailed kinetic parameters at aqueous interfaces, such as for Diels–Alder reactions at oil–water interfaces[221], this topic clearly deserves further insight from experiments and MD simulations taking into account finite thickness of the interface and solvent entropy.

Advanced molecular-dynamics simulations

A growing number of numerical simulations of reactions at aqueous interfaces have been performed in recent years using a variety of theoretical approaches. Some works have studied traditional organic reactions such as the Diels–Alder reaction[222,223], the Claisen rearrangement[224,225], the S_N2 reaction[226] and charge transfers[9,226,227]. Other works have looked at atmospheric reactions to study the role of cloud-water droplets on the photochemical production of OH radicals[7,188,228–230], acid dissociation[8,146–148,150,186,231] or other fundamental processes[6,20,232]. Intramolecular proton transfer of amino acids at water–hydrophobic interfaces has also been studied as a model for biological passive transport across cell membranes[233].

Ab initio MD is the most appropriate technique to study processes at the aqueous interfaces because of the possibility to describe the formation and breaking of chemical bonds, which is not possible to achieve at the same level of accuracy using, for example, classical force fields. Unfortunately, the computational cost required to obtain free-energy surfaces is very high, even when only part of the system is described quantum mechanically, as in combined quantum mechanics/molecular mechanics(QM/MM)[190] or perturbative dual-level[234] approaches. Moreover, in-depth studies require exploring the full reaction pathways and the low-probability regions of the activated complex, for example, through parallel rare-event sampling methods[235], replica path or nudged elastic-band methods[236]. As a consequence, most of the studies have been limited to short simulation times and/or approximate theoretical models and methods, focusing mainly on the calculation of equilibrium free energies, rather than on the study of dynamic reactive trajectories. In short, the simulation of chemical reactions at liquid-water interfaces can be considered still in its infancy, notwithstanding a few achievements of general interest and potential important relevance that we briefly comment on hereafter.

Thermal fluctuations of the solvent lay at the core of Marcus non-adiabatic theory of electron-transfer processes and Kramers–Grote–Hynes theory of reaction rates in solution, which introduces dynamical solvent effects by a generalized Langevin equation with a time-dependent solvent friction coefficient[213]. Ab initio QM/MM simulations have shown that the fluctuations spanned by solute–solvent dynamics at aqueous interfaces are at least comparable in magnitude to fluctuations in bulk[188].

Large thermal fluctuations at the air–water interface lead to the broadening of spectral bands, as experimentally observed in heterodyne-detected electronic SFG spectra of solvatochromic coumarins[237]. For example, broadening of ultraviolet–visible absorption bands may give rise to enhanced photochemistry in the troposphere. According to simulations, the production rate of OH radicals by the photolysis of ozone would be accelerated by four orders of magnitude when the process takes place at the surface of water droplets[188], and significant rate increase has also been predicted for other OH sources[228–230].

To date, very few studies have looked at reactive trajectories at interfaces and most have considered spontaneous processes with low energy barriers[150,231]. Fluctuations of the hydrogen-bond network are known to drive proton transfers in liquid water[238], whereas tunnelling may be important for proton mobility in other systems. The ab initio MD simulation of formic-acid deprotonation and subsequent proton transfer in the water medium through the Grotthuss mechanism[150] showed that proton transfer is controlled by fluctuations of water O⋯O distances, as in bulk water, and occurs when these distances shrink to ~2.4 Å. Most sequential events are separated by rest periods, and the whole process takes place in a few-picosecond timescale. A similar mechanism and O⋯O distance have been reported in QM/MM simulations for the deprotonation of the radical HOSO at the air–water interface[8].

Though tunnelling appears to be important only at low temperatures or high pressures in water, other nuclear quantum effects may be important at standard temperature and pressure conditions in bulk and at interfaces[239,240]. For example, Shrestha et al.[241] have recently shown that the attractive hydrophobic forces between perfluorinated surfaces in nanoconfinement are approximately 10% higher in H_2O than in D_2O, and have attributed this result to the contribution of zero-point energies. This finding encourages further experimental and theoretical studies that would enable us to assess the possible influence of these terms on on-water catalytic effects.

QM/MM MD simulations of $ClCH_3 + OH$ at the air–water interface have been performed, generating random trajectories from the transition state with a rare-event sampling technique[242] (FIG. 6). The method allows to estimate the number of recrossings of the activation barrier (which occur at short times, <20 fs) and the ratio between reactive and non-reactive trajectories (~29%), suggesting a significant dynamic solvation effect on the interfacial-reaction mechanism. This dynamic effect is arguably a general trend in interfacial chemical reactions, for which the timescales for solute's translational and rotational relaxation make the equilibrium hypothesis in transition-state theory questionable, though much work is still necessary to clarify this issue.

Concluding remarks

In this Review, we have presented and briefly discussed the current state of knowledge in the cross-cutting field of on-water catalysis. In the last fifteen years, from the first studies performed using stirred reactants in water suspensions[1,2] to the most recent experiments in
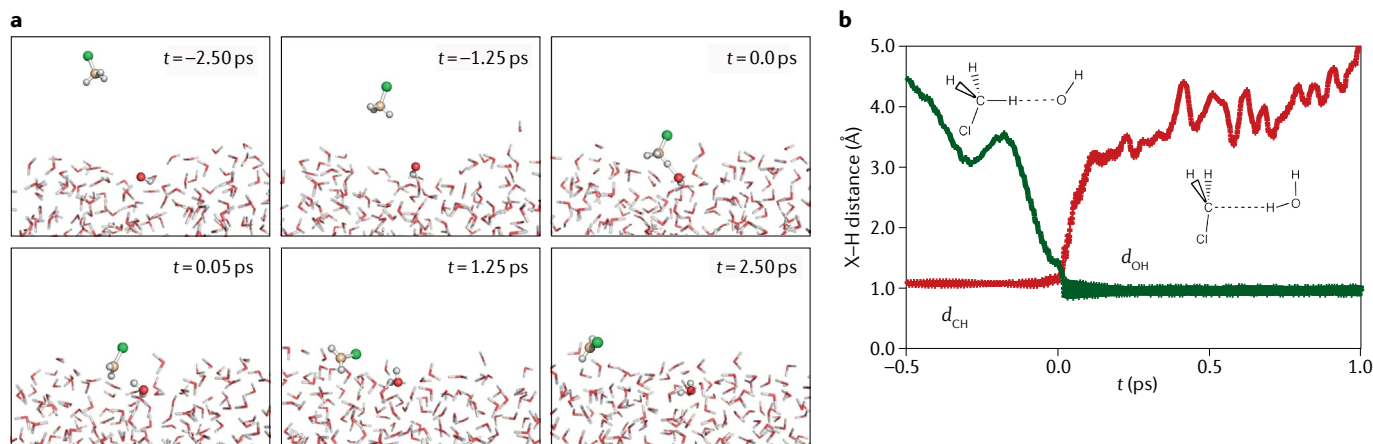
Fig. 6 | **Molecular-dynamics simulations of reactions at the air–water interface. a** | Snapshot of a CH_3Cl molecule in the gas phase that approaches the hydrated OH radical at the air–water interface and reacts with it to form the products on a short timescale. **b** | The reactive trajectory for the $CH_3Cl + OH \rightarrow CH_2Cl + H_2O$ reaction at the air–water interface has been obtained, performing a multiscale molecular-dynamics simulation using the rare-event sampling approach[242]. An approximated structure of the transition state is first sampled with a constrained reaction coordinate, and a set of solute–solvent configurations is selected for further analysis. From each transition-state configuration ($t = 0$), two half trajectories are propagated, forwards and backwards in time. The half trajectories are linked together: reactive trajectories are those connecting the reactants to the products. They are arbitrarily reorganized so that the reactants lie on the negative time side and the products on the positive time side. Only 29% of the calculated trajectories are reactive, indicating the existence of non-negligible dynamic solvent effects (the other trajectories connect reactants to reactants or products to products). Part **a** is adapted with permission from REF.[242], Wiley.

sprayed microdroplets[16,79,81,85], this notion has taken a great leap forward. The fact that many reactions are accelerated at the surface of water and aqueous interfaces has significant implications in atmospheric, environmental, biological or prebiotic chemistries, for example. At the same time, it opens up vast innovative avenues for the development of green processes in synthetic chemistry.

The catalytic effect of the water surface is still incompletely understood. However, considerable progress has been gained in recent years, in large part, because of the development of interface-sensitive spectroscopic techniques and detailed microscopic description achieved through advanced MD simulations. Rate acceleration can stem from solvation effects but also from intrinsic acid–base properties of the water surface, which differ from those in the bulk. The most evident solvation effect is the enhancement of the reactant concentrations at the interface, because neutral molecules and soft anions tend to stabilize there, favoured by enthalpic or entropic effects, and sometimes both. For the same reason, transition states can be stabilized, and experiments and calculations suggest that the activation energy of some reactions can be significantly lowered at the interface, compared with bulk. In this regard, it is definitely essential to clarify and quantify the effect of dangling –OH groups and surface electrostatic potentials, as well as the contribution of entropy changes, e.g. in bimolecular reactions. To this aim, ab initio MD simulation is a priceless tool, although further improvements of current techniques are needed. Simulations at the ab initio level represent a high computational cost. Therefore, their accuracy is generally limited by two main factors: too short simulation times and use of approximate quantum

methods. With consequences such as limited statistics and accuracy, current simulations cannot always capture the subtle properties of interfacial water molecules or the delicate balance of the energetics in a chemical reaction.

Future studies should clarify which catalytic processes are purely due to environmental effects and which are caused by other factors, such as the charge separation or gas-phase chemistry in electrospray experiments, or the diffuse interfaces of emulsions, owing to partial solubility in water (that is, what is the role of organic molecules in the aqueous phase and vice versa). There are two main avenues in this respect. First, rates of one reaction should be measured using different kinds of experiments. Second, simulations with more and more realistic models should be implemented. Quantum effects have generally been neglected in the calculations, but experiments have shown that they can play a significant role[239,241]. Among the pressing aspects that need a deeper understanding are: the role of electrostatic potential of the water surface, the autoionization kinetics and thermodynamics of water, or the distribution of ions in the interfacial layers. Another issue of great interest is the study of reactions at aqueous interfaces with non-organic solvents, such as ionic liquids or compressed CO_2, which are shaping up as possible candidates for developing new green synthetic methods. In parallel with progress in simulations and the emergence of new experimental set-ups, knowledge transfer between fields will be essential to meet all these challenges, which are of utmost relevance in various areas of science and technology.

REVIEWS

1. Narayan, S. et al. "On water": unique reactivity of organic compounds in aqueous suspension. *Angew. Chem. Int. Ed.* **44**, 3275–3279 (2005).

2. Jung, Y. & Marcus, R. A. On the theory of organic catalysis "on water". *J. Am. Chem. Soc.* **129**, 5492–5502 (2007).

3. Adamson, A. W. *Physical Chemistry of Surfaces* 5th edn (Wiley, 1990).

4. Donaldson, D. J. & Vaida, V. The influence of organic films at the air–aqueous boundary on atmospheric processes. *Chem. Rev.* **106**, 1445–1461 (2006).

5. Jubb, A. M., Hua, W. & Allen, H. C. Environmental chemistry at vapor/water interfaces: insights from vibrational sum frequency generation spectroscopy. *Annu. Rev. Phys. Chem.* **63**, 107–130 (2012).

6. Gerber, R. B. et al. Computational studies of atmospherically-relevant chemical reactions in water clusters and on liquid water and ice surfaces. *Acc. Chem. Res.* **48**, 399–406 (2015).

7. Zhong, J. et al. Atmospheric spectroscopy and photochemistry at environmental water interfaces. *Annu. Rev. Phys. Chem.* **70**, 45–69 (2019).

8. Ruiz-Lopez, M. F., Martins-Costa, M. T. C., Anglada, J. M. & Francisco, J. S. A new mechanism of acid rain generation from HOSO at the air–water interface. *J. Am. Chem. Soc.* **141**, 16564–16568 (2019).

9. Benjamin, I. Chemical reactions and solvation at liquid interfaces: A microscopic perspective. *Chem. Rev.* **96**, 1449–1475 (1996).

10. Jungwirth, P. & Tobias, D. J. Specific ion effects at the air/water interface. *Chem. Rev.* **106**, 1259–1281 (2006).

11. Finlayson-Pitts, B. J. Reactions at surfaces in the atmosphere: integration of experiments and theory as necessary (but not necessarily sufficient) for predicting the physical chemistry of aerosols. *Phys. Chem. Chem. Phys.* **11**, 7760–7779 (2009).

12. Donaldson, D. J. & Valsaraj, K. T. Adsorption and reaction of trace gas-phase organic compounds on atmospheric water film surfaces: a critical review. *Environ. Sci. Technol.* **44**, 865–873 (2010).

13. Valsaraj, K. T. A review of the aqueous aerosol surface chemistry in the atmospheric context. *Open J. Phys. Chem.* **2**, 17542 (2012).

14. George, C., Ammann, M., D'Anna, B., Donaldson, D. J. & Nizkorodov, S. A. Heterogeneous photochemistry in the atmosphere. *Chem. Rev.* **115**, 4218–4258 (2015).

15. Herrmann, H. et al. Tropospheric aqueous-phase chemistry: kinetics, mechanisms, and its coupling to a changing gas phase. *Chem. Rev.* **115**, 4259–4334 (2015).

16. Yan, X., Bain, R. M. & Cooks, R. G. Organic reactions in microdroplets: reaction acceleration revealed by mass spectrometry. *Angew. Chem. Int. Ed.* **55**, 12960–12972 (2016).

17. Butler, R. N. & Coyne, A. G. Organic synthesis reactions on-water at the organic-liquid water interface. *Org. Biomol. Chem.* **14**, 9945–9960 (2016).

18. Serrano-Luginbuhl, S., Ruiz-Mirazo, K., Ostaszewski, R., Gallou, F. & Walde, P. Soft and dispersed interface-rich aqueous systems that promote and guide chemical reactions. *Nat. Rev. Chem.* **2**, 306–327 (2018).

19. Ravishankara, A. R. Heterogeneous and multiphase chemistry in the troposphere. *Science* **276**, 1058–1065 (1997).

20. Knipping, E. M. et al. Experiments and simulations of ion-enhanced interfacial chemistry on aqueous NaCl aerosols. *Science* **288**, 301–306 (2000).

21. Rossignol, S. et al. Atmospheric photochemistry at a fatty acid–coated air-water interface. *Science* **353**, 699–702 (2016).

22. Banerjee, S. & Zare, R. N. Syntheses of isoquinoline and substituted quinolines in charged microdroplets. *Angew. Chem. Int. Ed.* **54**, 14795–14799 (2015).

23. Bain, R. M., Sathyamoorthi, S. & Zare, R. N. "On-droplet" chemistry: the cycloaddition of diethyl azodicarboxylate and quadricyclane. *Angew. Chem. Int. Ed.* **56**, 15083–15087 (2017).

24. Yan, X., Lai, Y. H. & Zare, R. N. Preparative microdroplet synthesis of carboxylic acids from aerobic oxidation of aldehydes. *Chem. Sci.* **9**, 5207–5211 (2018).

25. Kuchler, A., Yoshimoto, M., Luginbuhl, S., Mavelli, F. & Walde, P. Enzymatic reactions in confined environments. *Nat. Nanotechnol.* **11**, 409–420 (2016).

26. Vaida, V. Prebiotic phosphorylation enabled by microdroplets. *Proc. Natl Acad. Sci. USA* **114**, 12359–12361 (2017).

27. Nam, I., Nam, H. G. & Zare, R. N. Abiotic synthesis of purine and pyrimidine ribonucleosides in aqueous microdroplets. *Proc. Natl Acad. Sci. USA* **115**, 36–40 (2018).

28. Rosenfeld, D., Sherwood, S., Wood, R. & Donner, L. Climate effects of aerosol-cloud interactions. *Science* **343**, 379–380 (2014).

29. Calvert, J. G. et al. Chemical mechanisms of acid generation in the troposphere. *Nature* **317**, 27–35 (1985).

30. Solomon, S., Garcia, R. R., Rowland, F. S. & Wuebbles, D. J. On the depletion of Antarctic ozone. *Nature* **321**, 755–758 (1986).

31. Andreae, M. O. & Crutzen, P. J. Atmospheric aerosols: Biogeochemical sources and role in atmospheric chemistry. *Science* **276**, 1052–1058 (1997).

32. Ravishankara, A. R. & Longfellow, C. A. Reactions on tropospheric condensed matter. *Phys. Chem. Chem. Phys.* **1**, 5433–5441 (1999).

33. Jacob, D. J. Heterogeneous chemistry and tropospheric ozone. *Atmos. Environ.* **34**, 2131–2159 (2000).

34. Monod, A. & Carlier, P. Impact of clouds on the tropospheric ozone budget: direct effect of multiphase photochemistry of soluble organic compounds. *Atmos. Environ.* **33**, 4431–4446 (1999).

35. Reichardt, C. *Solvents and Solvent Effects in Organic Chemistry* 3rd edn (Wiley, 2003).

36. Kolb, C. E. et al. An overview of current issues in the uptake of atmospheric trace gases by aerosols and clouds. *Atmos. Chem. Phys.* **10**, 10561–10605 (2010).

37. Enami, S., Hoffmann, M. R. & Colussi, A. J. Extensive H-atom abstraction from benzoate by OH-radicals at the air–water interface. *Phys. Chem. Chem. Phys.* **18**, 31505–31512 (2016).

38. Enami, S., Mishra, H., Hoffmann, M. R. & Colussi, A. J. Protonation and oligomerization of gaseous isoprene on mildly acidic surfaces: implications for atmospheric chemistry. *J. Phys. Chem. A* **116**, 6027–6032 (2012).

39. Enami, S. & Colussi, A. J. Efficient scavenging of Criegee intermediates on water by surface-active cis-pinonic acid. *Phys. Chem. Chem. Phys.* **19**, 17044–17051 (2017).

40. Enami, S. & Colussi, A. J. Reactions of Criegee intermediates with alcohols at air–aqueous interfaces. *J. Phys. Chem. A* **121**, 5175–5182 (2017).

41. Enami, S., Hoffmann, M. R. & Colussi, A. J. Criegee intermediates react with levoglucosan on water. *J. Phys. Chem. Lett.* **8**, 3888–3894 (2017).

42. Qiu, J. T., Ishizuka, S., Tonokura, K., Colussi, A. J. & Enami, S. Reactivity of monoterpene Criegee intermediates at gas–liquid interfaces. *J. Phys. Chem. A* **122**, 7910–7917 (2018).

43. Qiu, J. T., Ishizuka, S., Tonokura, K. & Enami, S. Reactions of Criegee intermediates with benzoic acid at the gas/liquid interface. *J. Phys. Chem. A* **122**, 6303–6310 (2018).

44. Qiu, J. T., Ishizuka, S., Tonokura, K. & Enami, S. Interfacial vs bulk ozonolysis of nerolidol. *Environ. Sci. Technol.* **53**, 5750–5757 (2019).

45. Qiu, J. T. et al. Effects of pH on interfacial ozonolysis of alpha-terpineol. *J. Phys. Chem. A* **123**, 7148–7155 (2019).

46. Mmereki, B. T., Donaldson, D. J., Gilman, J. B., Eliason, T. L. & Vaida, V. Kinetics and products of the reaction of gas-phase ozone with anthracene adsorbed at the air–aqueous interface. *Atmos. Environ.* **38**, 6091–6103 (2004).

47. Thomas, J. L., Jimenez-Aranda, A., Finlayson-Pitts, B. J. & Dabdub, D. Gas-phase molecular halogen formation from NaCl and NaBr aerosols: When are interface reactions important? *J. Phys. Chem. A* **110**, 1859–1867 (2006).

48. Richards-Henderson, N. K. et al. Production of gas phase NO₂ and halogens from the photolysis of thin water films containing nitrate, chloride and bromide ions at room temperature. *Phys. Chem. Chem. Phys.* **15**, 17636–17646 (2013).

49. Richards, N. K. et al. Nitrate ion photolysis in thin water films in the presence of bromide ions. *J. Phys. Chem. A* **115**, 5810–5821 (2011).

50. Richards-Henderson, N. K., Anderson, C., Anastasio, C. & Finlayson-Pitts, B. J. The effect of cations on NO₂ production from the photolysis of aqueous thin water films of nitrate salts. *Phys. Chem. Chem. Phys.* **17**, 32211–32218 (2015).

51. Vaida, V. Perspective: water cluster mediated atmospheric chemistry. *J. Chem. Phys.* **135**, 020901 (2011).

52. Shrestha, M. et al. Let there be light: stability of palmitic acid monolayers at the air/salt water interface in the presence and absence of simulated solar light and a photosensitizer. *Chem. Sci.* **9**, 5716–5723 (2018).

53. Rapf, R. J. et al. Environmental processing of lipids driven by aqueous photochemistry of α-keto acids. *ACS Cent. Sci.* **4**, 624–630 (2018).

54. Reed Harris, A. E. et al. Multiphase photochemistry of pyruvic acid under atmospheric conditions. *J. Phys. Chem. A* **121**, 3327–3339 (2017).

55. Li, C. J. Organic reactions in aqueous media-with a focus on carbon-carbon bond formation. *Chem. Rev.* **93**, 2023–2035 (1993).

56. Gajewski, J. J. The Claisen rearrangement. Response to solvents and substituents: the case for both hydrophobic and hydrogen bond acceleration in water and for a variable transition state. *Acc. Chem. Res.* **30**, 219–225 (1997).

57. Lindström, U. M. Stereoselective organic reactions in water. *Chem. Rev.* **102**, 2751–2772 (2002).

58. Romney, D. K., Arnold, F. H., Lipshutz, B. H. & Li, C. J. Chemistry takes a bath: reactions in aqueous media. *J. Org. Chem.* **83**, 7319–7322 (2018).

59. Rideout, D. C. & Breslow, R. Hydrophobic acceleration of Diels-Alder reactions. *J. Am. Chem. Soc.* **102**, 7816–7817 (1980).

60. Breslow, R. Hydrophobic effects on simple organic reactions in water. *Acc. Chem. Res.* **24**, 159–164 (1991).

61. Butler, R. N., Coyne, A. G., Cunningham, W. J. & Moloney, E. M. Water and organic synthesis: a focus on the in-water and on-water border. Reversal of the in-water Breslow hydrophobic enhancement of the normal *endo*-effect on crossing to on-water conditions for Huisgen cycloadditions with increasingly insoluble organic liquid and solid 2π-dipolarophiles. *J. Org. Chem.* **78**, 3276–3291 (2013).

62. Augusti, R., Chen, H., Eberlin, L. S., Nefliu, M. & Cooks, R. G. Atmospheric pressure Eberlin transacetalization reactions in the heterogeneous liquid/gas phase. *Int. J. Mass. Spectrom.* **253**, 281–237 (2006).

63. Girod, M., Moyano, E., Campbell, D. I. & Cooks, R. G. Accelerated bimolecular reactions in microdroplets studied by desorption electrospray ionization mass spectrometry. *Chem. Sci.* **2**, 501–510 (2011).

64. Bain, R. M., Pulliam, C. J. & Cooks, R. G. Accelerated Hantzsch electrospray synthesis with temporal control of reaction intermediates. *Chem. Sci.* **6**, 397–401 (2015).

65. Bain, R. M., Ayrton, S. T. & Cooks, R. G. Fischer indole synthesis in the gas phase, the solution phase, and at the electrospray droplet interface. *J. Am. Soc. Mass. Spectrom.* **28**, 1359–1364 (2017).

66. Zhang, W. W., Yang, S. W., Lin, Q. Y., Cheng, H. Y. & Liu, J. H. Microdroplets as microreactors for fast synthesis of ketoximes and amides. *J. Org. Chem.* **84**, 851–859 (2019).

67. Sahota, N. et al. A microdroplet-accelerated Biginelli reaction: mechanisms and separation of isomers using IMS-MS. *Chem. Sci.* **10**, 4822–4827 (2019).

68. Bain, R. M., Pulliam, C. J., Thery, F. & Cooks, R. G. Accelerated chemical reactions and organic synthesis in Leidenfrost droplets. *Angew. Chem. Int. Ed.* **55**, 10478–10482 (2016).

69. Badu-Tawiah, A. K., Campbell, D. I. & Cooks, R. G. Reactions of microsolvated organic compounds at ambient surfaces: droplet velocity, charge state, and solvent effects. *J. Am. Soc. Mass. Spectrom.* **23**, 1077–1084 (2012).

70. Badu-Tawiah, A. K., Campbell, D. I. & Cooks, R. G. Accelerated C–N bond formation in dropcast thin films on ambient surfaces. *J. Am. Soc. Mass. Spectrom.* **23**, 1461–1468 (2012).

71. Song, H., Chen, D. L. & Ismagilov, R. F. Reactions in droplets in microfluidic channels. *Angew. Chem. Int. Ed.* **45**, 7336–7356 (2006).

72. Mashaghi, S. & van Oijen, A. M. External control of reactions in microdroplets. *Sci. Rep.* **5**, 11837 (2015).

73. Mellouli, S., Bousekkine, L., Theberge, A. B. & Huck, W. T. S. Investigation of "on water" conditions using a biphasic fluidic platform. *Angew. Chem. Int. Ed.* **51**, 7981–7984 (2012).

74. Fallah-Araghi, A. et al. Enhanced chemical synthesis at soft interfaces: A universal reaction-adsorption mechanism in microcompartments. *Phys. Rev. Lett.* **112**, 028301 (2014).

75. Banerjee, S., Gnanamani, E., Yan, X. & Zare, R. N. Can all bulk-phase reactions be accelerated in microdroplets? *Analyst* **142**, 1399–1402 (2017).

76. Li, Y., Yan, X. & Cooks, R. G. The role of the interface in thin film and droplet accelerated reactions studied by competitive substituent effects. *Angew. Chem. Int. Ed.* **55**, 3433–3437 (2016).

77. Lee, J. K., Banerjee, S., Nam, H. G. & Zare, R. N. Acceleration of reaction in charged microdroplets. *Q. Rev. Biophys.* **48**, 437–444 (2015).

78. Enami, S., Sakamoto, Y. & Colussi, A. J. Fenton chemistry at aqueous interfaces. *Proc. Natl Acad. Sci. USA* **111**, 623–628 (2014).

79. Lee, J. K. et al. Spontaneous generation of hydrogen peroxide from aqueous microdroplets. *Proc. Natl Acad. Sci. USA* **116**, 19294–19298 (2019).

80. Zhu, C. Q. & Francisco, J. S. Production of hydrogen peroxide enabled by microdroplets. *Proc. Natl Acad. Sci. USA* **116**, 19222–19224 (2019).

81. Gao, D., Jin, F., Lee, J. K. & Zare, R. N. Aqueous microdroplets containing only ketones or aldehydes undergo Dakin and Baeyer–Villiger reactions. *Chem. Sci.* **10**, 10974–10978 (2019).

82. Enami, S., Hoffmann, M. R. & Colussi, A. J. Acidity enhances the formation of a persistent ozonide at aqueous ascorbate/ozone gas interfaces. *Proc. Natl Acad. Sci. USA* **105**, 7365–7369 (2008).

83. Enami, S., Hoffmann, M. R. & Colussi, A. J. Ozonolysis of uric acid at the air/water interface. *J. Phys. Chem. B* **112**, 4153–4156 (2008).

84. Enami, S., Hoffmann, M. R. & Colussi, A. J. Simultaneous detection of cysteine sulfenate, sulfinate, and sulfonate during cysteine interfacial ozonolysis. *J. Phys. Chem. B* **113**, 9356–9358 (2009).

85. Liu, C. Y., Li, J., Chen, H. & Zare, R. N. Scale-up of microdroplet reactions by heated ultrasonic nebulization. *Chem. Sci.* **10**, 9367–9373 (2019).

86. Gallo, A. et al. The chemical reactions in electrosprays of water do not always correspond to those at the pristine air–water interface. *Chem. Sci.* **10**, 2566–2577 (2019).

87. Jacobs, M. I., Davis, R. D., Rapf, R. J. & Wilson, K. R. Studying chemistry in micro-compartments by separating droplet generation from ionization. *J. Am. Soc. Mass. Spectrom.* **30**, 339–343 (2019).

88. Bachmann, P. A., Luisi, P. L. & Lang, J. Autocatalytic self-replicating micelles as models for prebiotic structures. *Nature* **357**, 57–59 (1992).

89. Dobson, C. M., Ellison, G. B., Tuck, A. F. & Vaida, V. Atmospheric aerosols as prebiotic chemical reactors. *Proc. Natl Acad. Sci. USA* **97**, 11864–11868 (2000).

90. Tuck, A. The role of atmospheric aerosols in the origin of life. *Surv. Geophys.* **23**, 379–409 (2002).

91. Donaldson, D. J., Tervahattu, H., Tuck, A. F. & Vaida, V. Organic aerosols and the origin of life: an hypothesis. *Orig. Life Evol. Biosph.* **34**, 57–67 (2004).

92. Szostak, J. W. The narrow road to the deep past: in search of the chemistry of the origin of life. *Angew. Chem. Int. Ed.* **56**, 11037–11043 (2017).

93. Griffith, E. C., Shoemaker, R. K. & Vaida, V. Sunlight-initiated chemistry of aqueous pyruvic acid: building complexity in the origin of life. *Orig. Life Evol. Biosph.* **43**, 341–352 (2013).

94. Walde, P., Umakoshi, H., Stano, P. & Mavelli, F. Emergent properties arising from the assembly of amphiphiles. Artificial vesicle membranes as reaction promoters and regulators. *Chem. Commun.* **50**, 10177–10197 (2014).

95. Walde, P., Goto, A., Monnard, P.-A., Wessicken, M. & Luisi, P. L. Oparin's reactions revisited: enzymic synthesis of poly(adenylic acid) in micelles and self-reproducing vesicles. *J. Am. Chem. Soc.* **116**, 7541–7547 (1994).

96. Kamat, N. P., Tobé, S., Hill, I. T. & Szostak, J. W. Electrostatic localization of RNA to protocell membranes by cationic hydrophobic peptides. *Angew. Chem. Int. Ed.* **54**, 11735–11739 (2015).

97. Zepik, H., Rajamani, S., Maurel, M.-C. & Deamer, D. Oligomerization of thioglutamic acid: Encapsulated reactions and lipid catalysis. *Orig. Life Evol. Biosph.* **37**, 495–505 (2007).

98. Blocher, M., Liu, D., Walde, P. & Luisi, P. L. Liposome-assisted selective polycondensation of α-amino acids and peptides. *Macromolecules* **32**, 7332–7334 (1999).

99. Murillo-Sánchez, S., Beaufils, D., González Mañas, J. M., Pascal, R. & Ruiz-Mirazo, K. Fatty acids' double role in the prebiotic formation of a hydrophobic dipeptide. *Chem. Sci.* **7**, 3406–3413 (2016).

100. Tervahattu, H., Juhanoja, J. & Kupiainen, K. Identification of an organic coating on marine aerosol particles by TOF-SIMS. *J. Geophys. Res. Atmos.* **107**, ACH 18-1–ACH 18-7 (2002).

101. Tervahattu, H. et al. New evidence of an organic layer on marine aerosols. *J. Geophys. Res. Atmos.* **107**, AAC 1-1–AAC 1-8 (2002).

102. Griffith, E. C. & Vaida, V. In situ observation of peptide bond formation at the water–air interface. *Proc. Natl Acad. Sci. USA* **109**, 15697–15701 (2012).

103. Lee, J. K., Samanta, D., Nam, H. G. & Zare, R. N. Micrometer-sized water droplets induce spontaneous reduction. *J. Am. Chem. Soc.* **141**, 10585–10589 (2019).

104. Nam, I., Lee, J. K., Nam, H. G. & Zare, R. N. Abiotic production of sugar phosphates and uridine ribonucleoside in aqueous microdroplets. *Proc. Natl Acad. Sci. USA* **114**, 12396–12400 (2017).

105. Bondar, A.-N. & Lemieux, M. J. Reactions at biomembrane interfaces. *Chem. Rev.* **119**, 6162–6183 (2019).

106. Breslow, R. Biomimetic chemistry and artificial enzymes: catalysis by design. *Acc. Chem. Res.* **28**, 146–153 (1995).

107. Breslow, R. & Dong, S. D. Biomimetic reactions catalyzed by cyclodextrins and their derivatives. *Chem. Rev.* **98**, 1997–2012 (1998).

108. Raynal, M., Ballester, P., Vidal-Ferran, A. & van Leeuwen, P. Supramolecular catalysis. Part 2: artificial enzyme mimics. *Chem. Soc. Rev.* **43**, 1734–1787 (2014).

109. Kuah, E., Toh, S., Yee, J., Ma, Q. & Gao, Z. Q. Enzyme mimics: advances and applications. *Chem. Eur. J.* **22**, 8404–8430 (2016).

110. Bjerre, J., Rousseau, C., Marinescu, L. & Bols, M. Artificial enzymes, "Chemzymes": current state and perspectives. *Appl. Microbiol. Biotechnol.* **81**, 1–11 (2008).

111. Motherwell, W. B., Bingham, M. J. & Six, Y. Recent progress in the design and synthesis of artificial enzymes. *Tetrahedron* **22**, 4663–4686 (2001).

112. Stevenson, J. D. & Thomas, N. R. Catalytic antibodies and other biomimetic catalysts. *Nat. Prod. Rep.* **17**, 535–577 (2000).

113. Huang, Y. Y., Ren, J. S. & Qu, X. G. Nanozymes: classification, catalytic mechanisms, activity regulation, and applications. *Chem. Rev.* **119**, 4357–4412 (2019).

114. Liang, M. & Yan, X. Nanozymes: from new concepts, mechanisms, and standards to applications. *Acc. Chem. Res.* **52**, 2190–2200 (2019).

115. Frechet, J. M. J. Dendrimers and supramolecular chemistry. *Proc. Natl Acad. Sci. USA* **99**, 4782–4787 (2002).

116. Astruc, D., Boisselier, E. & Ornelas, C. Dendrimers designed for functions: from physical, photophysical, and supramolecular properties to applications in sensing, catalysis, molecular electronics, photonics, and nanomedicine. *Chem. Rev.* **110**, 1857–1959 (2010).

117. Dwars, T., Paetzold, E. & Oehme, G. Reactions in micellar systems. *Angew. Chem. Int. Ed.* **44**, 7174–7199 (2005).

118. Shultz, M. J., Vu, T. H., Meyer, B. & Bisson, P. Water: A responsive small molecule. *Acc. Chem. Res.* **45**, 15–22 (2012).

119. Du, Q., Superfine, R., Freysz, E. & Shen, Y. R. Vibrational spectroscopy of water at the vapor/water interface. *Phys. Rev. Lett.* **70**, 2313 (1993).

120. Wilson, M. A., Pohorille, A. & Pratt, L. R. Molecular-dynamics of the water liquid-vapor interface. *J. Phys. Chem.* **91**, 4873–4878 (1987).

121. Townsend, R. M. & Rice, S. A. Molecular dynamics studies of the liquid–vapor interface of water. *J. Chem. Phys.* **94**, 2207–2218 (1991).

122. Morita, A. & Hynes, J. T. A theoretical analysis of the sum frequency generation spectrum of the water surface. *Chem. Phys.* **258**, 371–390 (2000).

123. Sulpizi, M., Salanne, M., Sprik, M. & Gaigeot, M.-P. Vibrational sum frequency generation spectroscopy of the water liquid–vapor interface from density functional theory-based molecular dynamics simulations. *J. Phys. Chem. Lett.* **4**, 83–87 (2012).

124. Kuo, I. F. W. & Mundy, C. J. An ab initio molecular dynamics study of the aqueous liquid-vapor interface. *Science* **303**, 658–660 (2004).

125. Pezzotti, S., Galimberti, D. R. & Gaigeot, M.-P. 2D H-bond network as the topmost skin to the air–water interface. *J. Phys. Chem. Lett.* **8**, 3133–3141 (2017).

126. Kuo, I. F. W. et al. Structure and dynamics of the aqueous liquid–vapor interface: a comprehensive particle-based simulation study. *J. Phys. Chem. B* **110**, 3738–3746 (2006).

127. Verde, A. V., Bolhuis, P. G. & Campen, R. K. Statics and dynamics of free and hydrogen-bonded OH groups at the air/water interface. *J. Phys. Chem. B* **116**, 9467–9481 (2012).

128. Taylor, R. S., Dang, L. X. & Garrett, B. C. Molecular dynamics simulations of the liquid/vapor interface of SPC/E water. *J. Phys. Chem.* **100**, 11720–11725 (1996).

129. Laage, D. & Hynes, J. T. A molecular jump mechanism of water reorientation. *Science* **311**, 832–835 (2006).

130. Hsieh, C.-S. et al. Ultrafast reorientation of dangling OH groups at the air-water interface using femtosecond vibrational spectroscopy. *Phys. Rev. Lett.* **107**, 116102 (2011).

131. Xiao, S., Figge, F., Stirnemann, G., Laage, D. & McGuire, J. A. Orientational dynamics of water at an extended hydrophobic interface. *J. Am. Chem. Soc.* **138**, 5551–5560 (2016).

132. Björneholm, O. et al. Water at interfaces. *Chem. Rev.* **116**, 7698–7726 (2016).

133. Lee, C. Y., McCammon, J. A. & Rossky, P. The structure of liquid water at an extended hydrophobic surface. *J. Chem. Phys.* **80**, 4448–4455 (1984).

134. Striolo, A. From interfacial water to macroscopic observables: a review. *Adsorp. Sci. Technol.* **29**, 211–258 (2011).

135. Lee, S. H. & Rossky, P. J. A comparison of the structure and dynamics of liquid water at hydrophobic and hydrophilic surfaces—a molecular dynamics simulation study. *J. Chem. Phys.* **100**, 3334–3345 (1994).

136. Laage, D., Elsaesser, T. & Hynes, J. T. Water dynamics in the hydration shells of biomolecules. *Chem. Rev.* **117**, 10694–10725 (2017).

137. Tang, F. J. et al. Definition of free O–H groups of water at the air–water interface. *J. Chem. Theor. Comput.* **14**, 357–364 (2018).

138. Buch, V., Milet, A., Vácha, R., Jungwirth, P. & Devlin, J. P. Water surface is acidic. *Proc. Natl Acad. Sci. USA* **104**, 7342–7347 (2007).

139. Beattie, J. K., Djerdjev, A. M. & Warr, G. G. The surface of neat water is basic. *Faraday Discuss.* **141**, 31–39 (2008).

140. Petersen, P. B. & Saykally, R. J. Is the liquid water surface basic or acidic? Macroscopic vs. molecular-scale investigations. *Chem. Phys. Lett.* **458**, 255–261 (2008).

141. Mishra, H. et al. Brønsted basicity of the air–water interface. *Proc. Natl Acad. Sci. USA* **109**, 18679–18683 (2012).

142. Saykally, R. J. Air/water interface: two sides of the acid–base story. *Nat. Chem.* **5**, 82–84 (2013).

143. Agmon, N. et al. Protons and hydroxide ions in aqueous systems. *Chem. Rev.* **116**, 7642–7672 (2016).

144. Levinger, N. E. Water in confinement. *Science* **298**, 1722–1723 (2002).

145. Crans, D. C. & Levinger, N. E. The conundrum of pH in water nanodroplets: sensing pH in reverse micelle water pools. *Acc. Chem. Res.* **45**, 1637–1645 (2012).

146. Shamay, E. S., Buch, V., Parrinello, M. & Richmond, G. L. At the water's edge: nitric acid as a weak acid. *J. Am. Chem. Soc.* **129**, 12910–12911 (2007).

147. Wang, S. Z., Bianco, R. & Hynes, J. T. Depth-dependent dissociation of nitric acid at an aqueous surface: Car–Parrinello molecular dynamics. *J. Phys. Chem. A* **113**, 1295–1307 (2009).

148. Baer, M. D., Tobias, D. J. & Mundy, C. J. Investigation of interfacial and bulk dissociation of HBr, HCl, and HNO$_3$ using density functional theory-based molecular dynamics simulations. *J. Phys. Chem. C* **118**, 29412–29420 (2014).

149. Mishra, H. et al. Anions dramatically enhance proton transfer through aqueous interfaces. *Proc. Natl Acad. Sci. USA* **109**, 10228–10232 (2012).

150. Murdachaew, G., Nathanson, G. M., Gerber, R. B. & Halonen, L. Deprotonation of formic acid in collisions with a liquid water surface studied by molecular dynamics and metadynamics simulations. *Phys. Chem. Chem. Phys.* **18**, 29756–29770 (2016).

151. Griffith, E. C. & Vaida, V. Ionization state of l-phenylalanine at the air–water interface. *J. Am. Chem. Soc.* **135**, 710–716 (2013).

152. Petersen, M. K., Iyengar, S. S., Day, T. J. F. & Voth, G. A. The hydrated proton at the water liquid/vapor interface. *J. Phys. Chem. B* **108**, 14804–14806 (2004).

153. Enami, S., Hoffmann, M. R. & Colussi, A. J. Proton availability at the air/water interface. *J. Phys. Chem. Lett.* **1**, 1599–1604 (2010).

154. Tabe, Y., Kikkawa, N., Takahashi, H. & Morita, A. Surface acidity of water probed by free energy calculation for trimethylamine protonation. *J. Phys. Chem. C* **118**, 977–988 (2013).

155. Tse, Y. L. S., Chen, C., Lindberg, G. E., Kumar, R. & Voth, G. A. Propensity of hydrated excess protons and hydroxide anions for the air–water interface. *J. Am. Chem. Soc.* **137**, 12610–12616 (2015).

156. Wei, H. et al. Aerosol microdroplets exhibit a stable pH gradient. *Proc. Natl Acad. Sci. USA* **115**, 7272–7277 (2018).

157. Colussi, A. J. Can the pH at the air/water interface be different from the pH of bulk water? *Proc. Natl Acad. Sci. USA* **115**, E7887–E7887 (2018).

REVIEWS

158. Vikesland, P. J., Wei, H. R., Huang, Q. S., Guo, H. Y. & Marr, L. C. Reply to Colussi: Microdroplet interfacial pH, the ongoing discussion. *Proc. Natl Acad. Sci. USA* **115**, E7888–E7889 (2018).

159. Yamaguchi, S., Kundu, A., Sen, P. & Tahara, T. Communication: Quantitative estimate of the water surface pH using heterodyne-detected electronic sum frequency generation. *J. Chem. Phys.* **137**, 151101 (2012).

160. Hub, J. S. et al. Thermodynamics of hydronium and hydroxide surface solvation. *Chem. Sci.* **5**, 1745–1749 (2014).

161. Tabe, Y., Kikkawa, N., Takahashi, H. & Morita, A. Reply to "Comment on 'Surface acidity of water probed by free energy calculation for trimethylamine protonation'". *J. Phys. Chem. C* **118**, 2895 (2014).

162. Das, S., Bonn, M. & Backus, E. H. G. The surface activity of the hydrated proton is substantially higher than that of the hydroxide ion. *Angew. Chem. Int. Ed.* **58**, 15636–15639 (2019).

163. Enami, S., Stewart, L. A., Hoffmann, M. R. & Colussi, A. J. Superacid chemistry on mildly acidic water. *J. Phys. Chem. Lett.* **1**, 3488–3493 (2010).

164. Colussi, A. J. & Enami, S. Comment on "Surface acidity of water probed by free energy calculation for trimethylamine protonation". *J. Phys. Chem. C* **118**, 2894 (2014).

165. Colussi, A. J. & Enami, S. Comment on "The chemical reactions in electrosprays of water do not always correspond to those at the pristine air-water interface". *Chem. Sci.* **10**, 8253–8255 (2019).

166. Beattie, J. K. The intrinsic charge on hydrophobic microfluidic substrates. *Lab Chip* **6**, 1409–1411 (2006).

167. Kuo, J. L., Ciobanu, C. V., Ojamae, L., Shavitt, I. & Singer, S. J. Short H-bonds and spontaneous self-dissociation in (H₂O)₂₀: effects of H-bond topology. *J. Chem. Phys.* **118**, 3583–3588 (2003).

168. Torrent-Sucarrat, M., Ruiz-Lopez, M. F., Martins-Costa, M., Francisco, J. S & Anglada, J. M. Protonation of water clusters induced by hydroperoxyl radical surface adsorption. *Chem. Eur. J.* **17**, 5076–5085 (2011).

169. Gallo, A. Jr et al. Reply to the 'Comment on "The chemical reactions in electrosprays of water do not always correspond to those at the pristine air–water interface"'. *Chem. Sci.* **10**, 8256–8261 (2019).

170. Tomasi, J., Mennucci, B. & Cammi, R. Quantum mechanical continuum solvation models. *Chem. Rev.* **105**, 2999–3093 (2005).

171. Mozgawa, K., Mennucci, B. & Frediani, L. Solvation at surfaces and interfaces: a quantum-mechanical/continuum approach including nonelectrostatic contributions. *J. Phys. Chem. C* **118**, 4715–4725 (2014).

172. Kelly, C. P., Cramer, C. J. & Truhlar, D. G. Predicting adsorption coefficients at air–water interfaces using universal solvation and surface area models. *J. Phys. Chem. B* **108**, 12882–12897 (2004).

173. Martins-Costa, M. T. C. & Ruiz-Lopez, M. F. Solvation effects on electronic polarization and reactivity indices at the air–water interface: insights from a theoretical study of cyanophenols. *Theor. Chem. Acc.* **134**, 17 (2015).

174. Wang, H. F., Borguet, E. & Eisenthal, K. B. Generalized interface polarity scale based on second harmonic spectroscopy. *J. Phys. Chem. B* **102**, 4927–4932 (1998).

175. Sen, S., Yamaguchi, S. & Tahara, T. Different molecules experience different polarities at the air/water interface. *Angew. Chem. Int. Ed.* **48**, 6439–6442 (2009).

176. Steel, W. H. & Walker, R. A. Solvent polarity at an aqueous/alkane interface: the effect of solute identity. *J. Am. Chem. Soc.* **125**, 1132–1133 (2003).

177. Steel, W. H. & Walker, R. A. Measuring dipolar width across liquid–liquid interfaces with 'molecular rulers'. *Nature* **424**, 296–299 (2003).

178. Costa Cabral, B. J., Coutinho, K. & Canuto, S. A first-principles approach to the dynamics and electronic properties of *p*-nitroaniline in water. *J. Phys. Chem. A* **120**, 3878–3887 (2016).

179. Zhu, C. Q., Kais, S., Zeng, X. C., Francisco, J. S. & Gladich, I. Interfaces select specific stereochemical conformations: the isomerization of glyoxal at the liquid water interface. *J. Am. Chem. Soc.* **139**, 27–30 (2017).

180. Zhong, J. et al. Tuning the stereoselectivity and solvation selectivity at interfacial and bulk environments by changing solvent polarity: isomerization of glyoxal in

181. Liyana-Arachchi, T. P. et al. Molecular simulations of green leaf volatiles and atmospheric oxidants on air/water interfaces. *Phys. Chem. Chem. Phys.* **15**, 3583–3592 (2013).

182. Hub, J. S., Caleman, C. & van der Spoel, D. Organic molecules on the surface of water droplets - an energetic perspective. *Phys. Chem. Chem. Phys.* **14**, 9537–9545 (2012).

183. Vácha, R., Slavíček, P., Mucha, M., Finlayson-Pitts, B. J. & Jungwirth, P. Adsorption of atmospherically relevant gases at the air/water interface: free energy profiles of aqueous solvation of N₂, O₂, O₃, OH, H₂O, HO₂, and H₂O₂. *J. Phys. Chem. A* **108**, 11573–11579 (2004).

184. Roeselová, M., Vieceli, J., Dang, L. X., Garrett, B. C. & Tobias, D. J. Hydroxyl radical at the air–water interface. *J. Am. Chem. Soc.* **126**, 16308–16309 (2004).

185. Vieceli, J. et al. Molecular dynamics simulations of atmospheric oxidants at the air–water interface: solvation and accommodation of OH and O₃. *J. Phys. Chem. B* **109**, 15876–15892 (2005).

186. Martins-Costa, M. T. C., Anglada, J. M., Francisco, J. S. & Ruiz-Lopez, M. Reactivity of atmospherically relevant small radicals at the air–water interface. *Angew. Chem. Int. Ed.* **51**, 5413–5417 (2012).

187. Martins-Costa, M. T. C., Anglada, J. M., Francisco, J. S. & Ruiz-Lopez, M. F. Reactivity of volatile organic compounds at the surface of a water droplet. *J. Am. Chem. Soc.* **134**, 11821–11827 (2012).

188. Anglada, J. M., Martins-Costa, M., Ruiz-López, M. F. & Francisco, J. S. Spectroscopic signatures of ozone at the air–water interface and photochemistry implications. *Proc. Natl Acad. Sci. USA* **111**, 11618–11623 (2014).

189. Tobias, D. J., Stern, A. C., Baer, M. D., Levin, Y. & Mundy, C. J. Simulation and theory of ions at atmospherically relevant aqueous liquid-air interfaces. *Annu. Rev. Phys. Chem.* **64**, 339–359 (2013).

190. Martins-Costa, M. T. C. & Ruiz-López, M. F. in *Quantum Modeling of Complex Molecular Systems* (eds Rivail, J.-L., Ruiz-Lopez, M. F. & Assfeld, X.) 303–324 (Springer, 2015).

191. Donovan, M. A. et al. Ultrafast reorientational dynamics of leucine at the air–water interface. *J. Am. Chem. Soc.* **138**, 5226–5229 (2016).

192. Levin, Y. & dos Santos, A. P. Ions at hydrophobic interfaces. *J. Phys. Condens. Matt.* **26**, 203101 (2014).

193. Sun, L., Li, X., Tu, Y. Q. & Agren, H. Origin of ion selectivity at the air/water interface. *Phys. Chem. Chem. Phys.* **17**, 4311–4318 (2015).

194. Onsager, L. & Samaras, N. N. T. The surface tension of Debye-Hückel electrolytes. *J. Chem. Phys.* **2**, 528–536 (1934).

195. Markin, V. S. & Volkov, A. G. Quantitative theory of surface tension and surface potential of aqueous solutions of electrolytes. *J. Phys. Chem. B* **106**, 11810–11817 (2002).

196. Petersen, P. B. & Saykally, R. J. On the nature of ions at the liquid water surface. *Annu. Rev. Phys. Chem.* **57**, 333–364 (2006).

197. Netz, R. R. & Horinek, D. Progress in modeling ion effects at the vapor/water interface. *Annu. Rev. Phys. Chem.* **63**, 401–418 (2012).

198. Wise, P. K. & Ben-Amotz, D. Interfacial adsorption of neutral and ionic solutes in a water droplet. *J. Phys. Chem. B* **122**, 3447–3453 (2018).

199. Jungwirth, P. & Winter, B. Ions at aqueous interfaces: from water surface to hydrated proteins. *Annu. Rev. Phys. Chem.* **59**, 343–366 (2008).

200. Levin, Y., dos Santos, A. P. & Diehl, A. Ions at the air-water interface: an end to a hundred-year-old mystery? *Phys. Rev. Lett.* **103**, 257802 (2009).

201. Otten, D. E., Shaffer, P. R., Geissler, P. L. & Saykally, R. J. Elucidating the mechanism of selective ion adsorption to the liquid water surface. *Proc. Natl Acad. Sci. USA* **109**, 701–705 (2012).

202. Duignan, T. T., Parsons, D. F. & Ninham, B. W. Ion interactions with the air–water interface using a continuum solvent model. *J. Phys. Chem. B* **118**, 8700–8710 (2014).

203. Wang, R. & Wang, Z. G. Continuous self-energy of ions at the dielectric interface. *Phys. Rev. Lett.* **112**, 136101 (2014).

204. Sagar, D. M., Bain, C. D. & Verlet, J. R. R. Hydrated electrons at the water/air interface. *J. Am. Chem. Soc.* **132**, 6917–6919 (2010).

205. Siefermann, K. R. et al. Binding energies, lifetimes and implications of bulk and interface solvated electrons in water. *Nat. Chem.* **2**, 274–279 (2010).

206. Gaiduk, A. P., Pham, T. A., Govoni, M., Paesani, F. & Galli, G. Electron affinity of liquid water. *Nat. Commun.* **9**, 247 (2018).

207. Ben-Amotz, D. Interfacial solvation thermodynamics. *J. Phys. Condens. Matt.* **28**, 414013 (2016).

208. Tong, Y., Zhang, I. Y. & Campen, R. K. Experimentally quantifying anion polarizability at the air/water interface. *Nat. Commun.* **9**, 1313 (2018).

209. Cheng, J., Vecitis, C. D., Hoffmann, M. R. & Colussi, A. J. Experimental anion affinities for the air/water interface. *J. Phys. Chem. B* **110**, 25598–25602 (2006).

210. Beck, T. L. The influence of water interfacial potentials on ion hydration in bulk water and near interfaces. *Chem. Phys. Lett.* **561**, 1–13 (2013).

211. Kathmann, S. M., Kuo, I. F. W. & Mundy, C. J. Electronic effects on the surface potential at the vapor–liquid interface of water. *J. Am. Chem. Soc.* **130**, 16556–16561 (2008).

212. Caleman, C., Hub, J. S., van Maaren, P. J. & van der Spoel, D. Atomistic simulation of ion solvation in water explains surface preference of halides. *Proc. Natl Acad. Sci. USA* **108**, 6838–6842 (2011).

213. Henriksen, N. E. & Hansen, F. Y. *Theories of Molecular Reaction Dynamics. The Microscopic Foundation of Chemical Kinetics* (Oxford Univ. Press, 2008).

214. Jung, Y. S. & Marcus, R. A. Protruding interfacial OH groups and 'on-water' heterogeneous catalysis. *J. Phys. Condens. Matt.* **22**, 284117 (2010).

215. Beattie, J. K., McErlean, C. S. P. & Phippen, C. B. W. The mechanism of on-water catalysis. *Chem. Eur. J.* **16**, 8972–8974 (2010).

216. Meir, R., Chen, H., Lai, W. Z. & Shaik, S. Oriented electric fields accelerate Diels–Alder reactions and control the *endo/exo* selectivity. *ChemPhysChem* **11**, 301–310 (2010).

217. Aragones, A. C. et al. Electrostatic catalysis of a Diels–Alder reaction. *Nature* **531**, 88–91 (2016).

218. Ruiz-López, M. F., Assfeld, X., García, J. I., Mayoral, J. A. & Salvatella, L. Solvent effects on the mechanism and selectivities of asymmetric Diels-Alder reactions. *J. Am. Chem. Soc.* **115**, 8780–8787 (1993).

219. Geerlings, P., De Proft, F. & Langenaeker, W. Conceptual density functional theory. *Chem. Rev.* **103**, 1793–1874 (2003).

220. MacRitchie, F. *Chemistry at Interfaces* (Academic, 1990).

221. Manna, A. & Kumar, A. Why does water accelerate organic reactions under heterogeneous condition? *J. Phys. Chem. A* **117**, 2446–2454 (2013).

222. Thomas, L. L., Tirado-Rives, J. & Jorgensen, W. L. Quantum mechanical/molecular mechanical modeling finds Diels–Alder reactions are accelerated less on the surface of water than in water. *J. Am. Chem. Soc.* **132**, 3097–3104 (2010).

223. Karhan, K., Khaliullin, R. Z. & Kuhne, T. D. On the role of interfacial hydrogen bonds in "on-water" catalysis. *J. Chem. Phys.* **141**, 22D528 (2014).

224. Acevedo, O. & Armacost, K. Claisen rearrangements: insight into solvent effects and "on water" reactivity from QM/MM simulations. *J. Am. Chem. Soc.* **132**, 1966–1975 (2010).

225. Zheng, Y. Y. & Zhang, J. P. Catalysis in the oil droplet/water interface for aromatic Claisen rearrangement. *J. Phys. Chem. A* **114**, 4325–4333 (2010).

226. Benjamin, I. Reaction dynamics at liquid interfaces. *Annu. Rev. Phys. Chem.* **66**, 165–188 (2015).

227. Vöhringer-Martinez, E. & Toro-Labbé, A. The mean reaction force: a method to study the influence of the environment on reaction mechanisms. *J. Chem. Phys.* **135**, 064505 (2011).

228. Martins-Costa, M. T. C., Anglada, J. M., Francisco, J. S. & Ruiz-López, M. F. Impacts of cloud water droplets on the OH production rate from peroxide photolysis. *Phys. Chem. Chem. Phys.* **19**, 31621–31627 (2017).

229. Martins-Costa, M. T. C., Anglada, J. M., Francisco, J. S. & Ruiz-López, M. F. Photochemistry of SO₂ at the air–water interface: a source of OH and HOSO radicals. *J. Am. Chem. Soc.* **140**, 12341–12344 (2018).

230. Martins-Costa, M. T. C., Anglada, J. M., Francisco, J. S. & Ruiz-López, M. F. Theoretical investigation of the photoexcited NO₂+H₂O reaction at the air–water interface and its atmospheric implications. *Chem. Eur. J.* **25**, 13899–13904 (2019).

231. Partanen, L., Murdachaew, G., Gerber, R. B. & Halonen, L. Temperature and collision energy effects on dissociation of hydrochloric acid on water surfaces. *Phys. Chem. Chem. Phys.* **18**, 13432–13442 (2016).

232. Colussi, A. J. et al. Tropospheric aerosol as a reactive intermediate. *Faraday Discuss.* **165**, 407–420 (2013).
233. Martins-Costa, M. T. C. & Ruiz-Lopez, M. F. Amino acid capture by aqueous interfaces. Implications for biological uptake. *J. Phys. Chem. B* **117**, 12469–12474 (2013).
234. Martins-Costa, M. T. C. & Ruiz-López, M. F. Highly accurate computation of free energies in complex systems through *horsetail* QM/MM molecular dynamics combined with free-energy perturbation theory. *Theor. Chem. Acc.* **136**, 50 (2017).
235. Strnad, M. et al. Molecular dynamics simulations of elementary chemical processes in liquid water using combined density functional and molecular mechanics potentials. II. Charge separation processes. *J. Chem. Phys.* **106**, 3643–3657 (1997).
236. Woodcock, H. L. III et al. Interfacing Q-Chem and CHARMM to perform QM/MM reaction path calculations. *J. Comput. Chem.* **28**, 1485–1502 (2007).
237. Mondal, S. K., Yamaguchi, S. & Tahara, T. Molecules at the air/water interface experience a more inhomogeneous solvation environment than in bulk solvents: a quantitative band shape analysis of interfacial electronic spectra obtained by HD-ESFG. *J. Phys. Chem. C* **115**, 3083–3089 (2011).
238. Ohmine, I. & Saito, S. Water dynamics: fluctuation, relaxation, and chemical reactions in hydrogen bond network rearrangement. *Acc. Chem. Res.* **32**, 741–749 (1999).
239. Ceriotti, M. et al. Nuclear quantum effects in water and aqueous systems: experiment, theory, and current challenges. *Chem. Rev.* **116**, 7529–7550 (2016).
240. Pereyaslavets, L. et al. On the importance of accounting for nuclear quantum effects in ab initio calibrated force fields in biological simulations. *Proc. Natl Acad. Sci. USA* **115**, 8878–8882 (2018).
241. Shrestha, B. R. et al. Nuclear quantum effects in hydrophobic nanoconfinement. *J. Phys. Chem. Lett.* **10**, 5530–5535 (2019).
242. Martins-Costa, M. T. C., Anglada, J. M. & Ruiz-López, M. F. Computational insights into the CH_3Cl+OH chemical reaction dynamics at the air–water interface. *ChemPhysChem* **18**, 2747–2755 (2017).

Publisher's note
Springer Nature remains neutral with regard to jurisdictional claims in published maps and institutional affiliations.